Geochemistry, Geophysics, Geosystems®

Key Points:

- Fossil-bound organic matter is well protected by the mineral matrix from chemical changes in the surrounding environment
- Partial dissolution of fossil calcite, aragonite, opal, and enamel has a negligible effect on their N isotopic composition and N content
- During heating, fossil N content and isotopic composition remains unchanged if the structure of the inorganic matrix is not compromised

Laboratory Assessment of the Impact of Chemical Oxidation, Mineral Dissolution, and Heating on the Nitrogen Isotopic Composition of Fossil-Bound Organic Matter

Alfredo Martínez-García[1] , **Jonathan Jung[1]** , **Xuyuan E. Ai[1,2]** , **Daniel M. Sigman[2]** , **Alexandra Auderset[1]** , **Nicolas N. Duprey[1]** , **Alan Foreman[1]** , **François Fripiat[1,3]** , **Jennifer Leichliter[1]** , **Tina Lüdecke[1]** , **Simone Moretti[1]** , and **Tanja Wald[1]**

[1]Max Planck Institute for Chemistry, Mainz, Germany, [2]Princeton University, Princeton, NJ, USA, [3]Université Libre de Bruxelles, Brussels, Belgium

Abstract Fossil-bound organic material holds great potential for the reconstruction of past changes in nitrogen (N) cycling. Here, with a series of laboratory experiments, we assess the potential effect of oxidative degradation, fossil dissolution, and thermal alteration on the fossil-bound N isotopic composition of different fossil types, including deep and shallow water scleractinian corals, foraminifera, diatoms and tooth enamel. Our experiments show that exposure to different oxidizing reagents does not significantly affect the N isotopic composition or N content of any of the fossil types analyzed, demonstrating that organic matter is well protected from changes in the surrounding environment by the mineral matrix. In addition, we show that partial dissolution (of up to 70%–90%) of fossil aragonite, calcite, opal, or enamel matrixes has a negligible effect on the N isotopic composition and N content of the fossils. These results suggest that the isotopic composition of fossil-bound organic material is relatively uniform, and also that N exposed during dissolution is lost without significant isotopic discrimination. Finally, our heating experiments show negligible changes in the N isotopic composition and N content of all fossil types at 100°C. At 200°C and hotter, any N loss and associated nitrogen isotope changes appear to be directly linked to the sensitivity of the mineral matrix to thermal stress, which depends on the biomineral type. These results suggest that, so long as high temperature does not compromise the mineral structure, the biomineral matrix acts as a closed system with respect to N, and the N isotopic composition of the fossil remains unchanged.

Plain Language Summary The ratio of the heavy and light isotopes of nitrogen (^{15}N and ^{14}N) in the organic material contained within the mineral structure of fossils can be used to reconstruct past changes in biological and chemical processes. With a series of laboratory experiments, we evaluate the potential effects of chemical conditions, fossil dissolution, and heating on the nitrogen isotopic composition ($^{15}N/^{14}N$ ratio) of corals, foraminifera, diatoms and tooth enamel. Our results indicate that these processes do not have a significant effect on the $^{15}N/^{14}N$ of fossils, suggesting that the mineral matrix provides a barrier that isolates a fossil's organic nitrogen from the surrounding environment, preventing alteration of its $^{15}N/^{14}N$. In addition, we show that if part of the fossil-bound organic nitrogen is exposed by dissolution or heating, it is lost without affecting the $^{15}N/^{14}N$ of the organic material that remains in the mineral. These findings imply that the original $^{15}N/^{14}N$ ratio incorporated by the organism is preserved in the geologic record. Therefore, measurements of the nitrogen isotopes on fossils can provide faithful biological, ecological, and environmental information about the past.

1. Introduction

The stable isotopes of nitrogen (^{14}N and ^{15}N) can offer important insights into present and past changes in the cycling of this key element through organisms, food webs, and environments (Casciotti, 2016; Deniro & Epstein, 1981; Fripiat et al., 2021; Sigman & Fripiat, 2019; Straub et al., 2021; Wolf et al., 2009). Their use in paleo-reconstructions requires the development of faithful geochemical archives that are unaffected by diagenetic alteration and/or contamination by exogenous N. In recent years, the analysis of the N isotopic composition of the organic matter bound within the mineral structure of fossil skeletons (e.g., foraminifera, corals, diatoms, otoliths, and tooth enamel) has emerged as a promising archive of the original isotopic signature of the organism that is protected from degradation for thousands to millions of years (Ai et al., 2020; Altabet & Curry, 1989;

Duprey et al., 2020; Erler et al., 2016, 2020; Farmer et al., 2021; Kast et al., 2019, 2022; Leichliter et al., 2021; Lueders-Dumont et al., 2018; Martinez-Garcia et al., 2014; Ren et al., 2009, 2017; Robinson et al., 2004, 2005; Shemesh et al., 1993; Sigman et al., 1999, 2021; Straub et al., 2013; Studer et al., 2015, 2018, 2021; Wang et al., 2014, 2016, 2017).

The compounds that comprise fossil-bound organic matter play an active, but still poorly understood, physiological role in the biomineralization process. In planktonic foraminifera and stony corals, this organic matter consists of a suite of proteins and polysaccharides that regulate the calcification process (Cusack & Freer, 2008; Ingalls et al., 2003; Weiner & Erez, 1984), with recent suggestions of a lipid component as well (Swart et al., 2021). In enamel, a group of specific proteins (amelogenin, enamelin, amelotin, and ameloblastin) play a key role as the structural scaffolds that determine mineral morphology during enamel development (Bai et al., 2020; Castiblanco et al., 2015). Although most of these organic compounds are digested and removed at the enamel maturation stage to achieve maximum hardness, these specific proteins are still found in tooth enamel samples that are millions of years old (Cappellini et al., 2019). In diatoms, frustule-bound organic matter is composed mainly of a set of taxon-specific polyamines and silaffins that promote silica precipitation during the formation of the diatom frustule (Bridoux, Annenkov et al., 2012, Bridoux, Keil et al., 2012; Kroger, 2002; Kroger et al., 2000). Fossil-bound organic material is, therefore, native to the organism.

Several lines of evidence suggest that the mineral matrix provides an effective barrier that protects the native, fossil-bound organic matter from contamination by external organic material from the surrounding sedimentary environment. For example, the amino acid composition of fossil-bound organic matter has significant differences from cooccurring organic matter in the sedimentary environment. The non-proteinogenic amino acids β-alanine and γ-aminobutyric are formed by microbial decarboxylation of aspartic and glutamic acids, making them ubiquitously abundant in marine sediments (Cowie & Hedges, 1994; Dauwe & Middelburg, 1998; Whelan, 1977). Thus, the absence of these amino acids in foraminifera tests suggests that the mineral matrix provides an effective barrier against microbial attack of fossil-bound organic matter and prevents the exchange of compounds with the surrounding sediments (Schroeder, 1975). In addition, laboratory studies indicate that the racemization reaction proceeds without significant impact on the nitrogen and carbon isotopic composition of the *D*- and *L*-enantiomers, so that the isotopic comparison of the enantiomers can be used to assess contamination of fossil-bound organic material (Engel & Macko, 1986). For example, the similarity of the carbon isotopic compositions of the *D*- and *L*-enantiomers of several individual amino acids in late Pleistocene land snail shells confirmed that their shell-bound amino acids were endogenous to the fossil (Engel et al., 1994). Finally, new biochemical and molecular biological tools are beginning to be applied to fossil-bound organic matter and speak to its fossil-native origin. For example, a recent analysis a 1.77 Ma extinct Rhinoceros tooth has shown that its enamel proteome is endogenous and almost complete (Cappellini et al., 2019).

The issue of endogeneity aside, there is also the possibility of effects of oxidative degradation, mineral dissolution, and thermal alteration on the N isotopic composition of fossil-bound organic material. Chemical and biological degradation are common in marine sediments and other environments (Arndt et al., 2013) and can alter substantially the original nitrogen isotopic composition of sedimentary organic matter (Robinson et al., 2012). A key postulate in the application of the fossil-bound N isotope method is that the mineral matrix provides an effective physical barrier that isolates organic compounds from the surrounding environment, protecting them from both external contamination and chemical or biological attack. The relative stability of the N content per mg of mineral of different fossil types (e.g., planktonic foraminifera, diatoms, scleractinian corals and tooth enamel) of the same species/genus over thousands and even millions of years supports this postulate (Kast et al., 2019; Leichliter et al., 2021; Ren et al., 2017; Studer et al., 2012; Wang et al., 2017). However, the stability of fossil-bound N isotopic composition under external chemical conditions that could favor organic matter degradation has not been systematically assessed.

Dissolution of calcium carbonate and opal is a widespread phenomenon in the ocean and other sedimentary systems (Sulpis et al., 2021; Van Cappellen et al., 2002). Partial dissolution of fossil mineral structures can substantially impact many geochemical proxies that rely on the isotopic and/or elemental composition of the inorganic biomineral matrix. These effects are thought to derive largely from the preferential dissolution of parts of the biomineral that have a distinct elemental or isotopic composition (Brown & Elderfield, 1996; McCorkle et al., 1995; Pearson, 2017; Rosenthal et al., 2000; Smith et al., 2016). In contrast, dissolution is thought to have a minimal effect on the N isotopic composition of organic matter bound within the biomineral structure of the

Table 1
Description of the Sample Materials Analyzed in This Study

MPIC-ID	Description/genus/species	Matrix	Location	Age	Reference
MF-1	Mixed Foraminifera, 63–315 μm size fraction	Calcite	North Atlantic	Late Holocene	This study
MF-2	Mixed Foraminifera, 63–315 μm size fraction	Calcite	Southern Ocean	Late Holocene	This study
PO-1	*Porites species*	Aragonite	Chuuk, Micronesia	Modern	Leichliter et al. (2021)
LO-1	*Lophelia pertusa*	Aragonite	North Atlantic	Modern	Leichliter et al. (2021)
AG-Lox	*Loxodonta africana*	Enamel	Africa	Modern	Gehler et al. (2012); Leichliter et al. (2021)
Noto-2	*Notochoerus scotti*	Enamel	Malawi, Africa	2.3–2.5 Ma	Kullmer (2008); Leichliter et al. (2021)
Hippo-1	*Hippopotamus amphibius*	Enamel	Malawi, Africa	1.8–3.75 Ma	This study
DI-1	Diatoms, <63 μm size fraction	Opal	Southern Ocean, core PS75/72-2	MIS11 (374–424 ka)	This study
DI-2	Diatoms, <63 μm size fraction	Opal	Southern Ocean, core PS69/899-2	MIS 5 (120–124 ka)	This study

fossils because: (a) the organic matter exposed after dissolution should ultimately be degraded and/or removed during cleaning prior to analysis (see Section 2.3), and (b) no reason is known for the isotopic composition of fossil-bound organic matter to vary coherently with dissolution susceptibility across the biomineral structure (Smart et al., 2018). However, so far, these two arguments have not been tested.

In addition, sedimentary organic matter degradation can increase during burial as a consequence of the temperature rise associated with local geothermal gradients, potentially causing important impacts on its molecular and isotopic composition (Burdige, 2006). Although typical temperatures in buried Cenozoic marine sediments are relatively low (<60°C) (Malinverno & Martinez, 2015), they can be substantially larger (>500°C) in other depositional settings that contain identifiable fossils (Rejebian et al., 1987). In any case, the potential effect of thermal degradation on the N isotopic composition of fossil-bound organic matter has not been examined.

In this study, we report results from laboratory experiments designed to evaluate the potential effects of oxidizing conditions, mineral dissolution, and thermal alteration on the nitrogen isotopic composition of fossil-bound organic matter.

2. Materials and Methods

2.1. Sample Materials

The different experiments were performed using a series of sample materials prepared at the Max Plank Institute for Chemistry (MPIC) in Mainz, Germany. These materials are intended to be representative of different fossil types typically used in paleo-reconstructions (Table 1) and include: modern deep-sea (*Lophelia pertusa, LO-1*) and shallow water (*Porites species, PO-1*) coral samples; late Holocene mixed foraminifera fractions (63–315 μm) from sediment cores collected in the North Atlantic (MF-1) and the Southern Ocean (MF-2); modern tooth enamel from an African elephant (*Loxodonta africana,* AG-Lox); fossil enamel from a Pleistocene (ca. 2.5–2.3 Ma) suid (*Notochoerus scotti*, Noto-2) from Zone 3A-2 of the Chiwondo Beds in Malawi (prepared from the same tooth as "Noto-1" reported in Leichliter et al. (2021)); fossil enamel from a Plio-Pleistocene (ca. 3.75–1.8 Ma) hippopotamus (*Hippopotamus amphibius,* Hippo-1) from Unit 3 at the Chiwondo Beds in Malawi; and two diatom samples obtained from sediment cores from the Antarctic Zone of the Southern Ocean (DI-1 and DI-2) prepared following the diatom separation methods described in Studer et al. (2015).

2.2. Experimental Design

The experimental design is summarized in Figure 1, and the different steps followed in each experiment are described below and in the next sections. For each sample type, an aliquot of uncleaned powder was taken and used in our chemical oxidation experiment. The remaining powder was subsequently cleaned in four aliquots (of
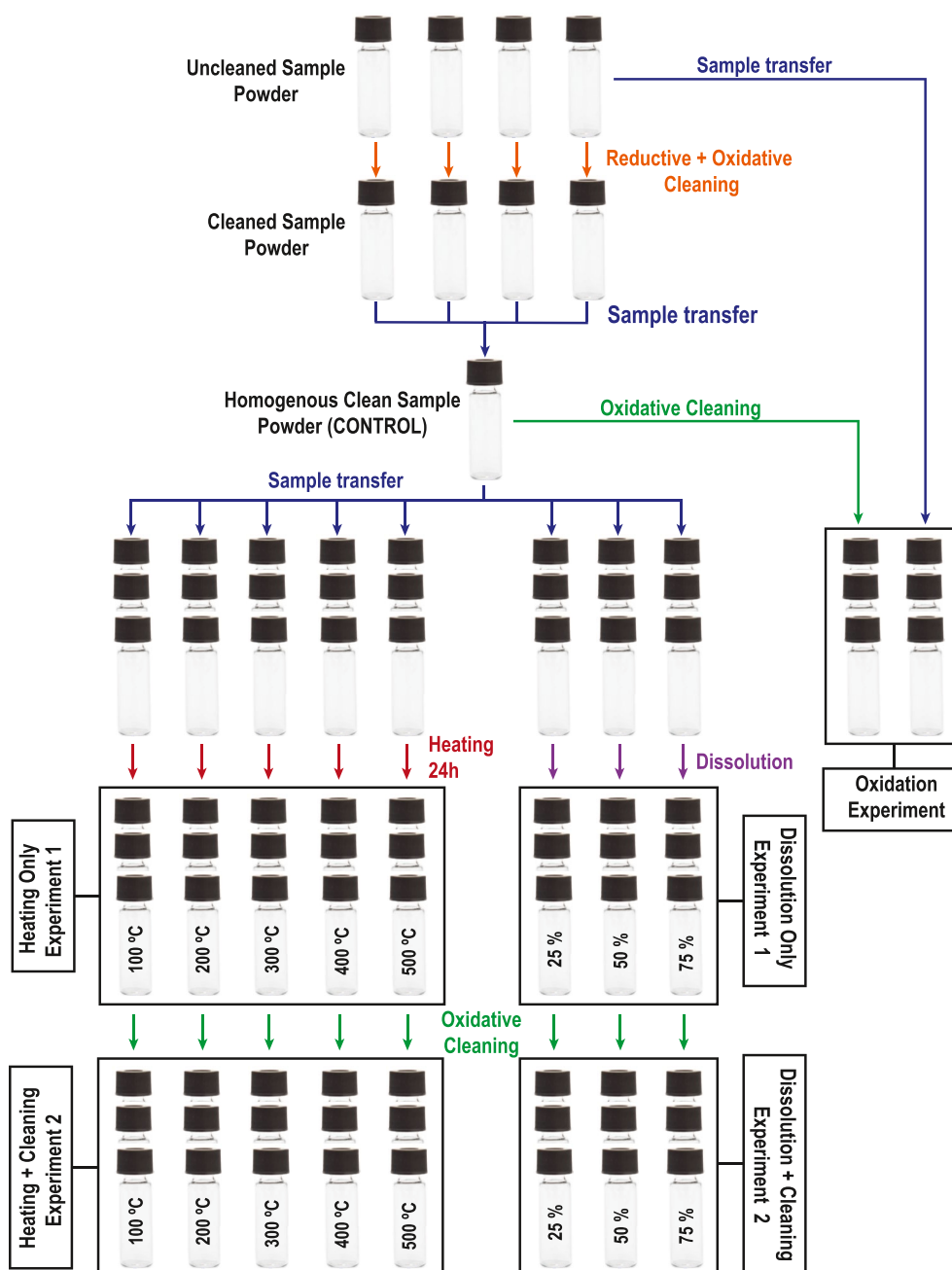
Figure 1. Experimental Design. For each sample type, an aliquot of uncleaned powder was taken and used in our chemical oxidation experiment. The remaining powder was subsequently cleaned in four aliquots (of 50 mg each) following the reductive-oxidative cleaning methods described in Section 2.3. After the cleaning, the dry fossil powder was combined in a single vial and homogenized. This homogenous, cleaned powder was measured (at least in triplicate) and used as a control sample for all of our treatments. In our oxidation experiment, the uncleaned sample aliquot was measured in triplicate and compared to our (cleaned) control sample, and to an aliquot of the control sample that was divided in triplicate, oxidatively cleaned for a second time, and measured. In our dissolution experiments, we performed three triplicate treatments in which approximately 25%, 50%, and 75% of the control sample was dissolved. In our first dissolution experiment, the sample powders remaining after dissolution were rinsed five times with Milli-Q water and measured. In our second experiment, the powders were recleaned oxidatively before measurement. In our heating experiments, the control sample powder was heated to 100°C, 200°, 300°, 400°, and 500°C. In our first experiment, samples were measured directly after heating; in our second experiment, samples were recleaned oxidatively before the measurement.

50 mg each) following the reductive-oxidative cleaning methods described in Section 2.3. After cleaning, the dry fossil powder was combined in a single vial and homogenized. This homogenous cleaned powder was measured (at least in triplicate) and used as a control sample for all our treatments. For both the dissolution and the thermal degradation experiments, samples were measured twice: (a) directly after the treatment, and (b) with a recleaning of the fossil powders after the dissolution and temperature treatments.

Each treatment was performed in triplicate for all the fossil standards described in Table 1. We performed a total of 413 individual measurements. The data are available in Data Set S1 in Supporting Information S1.

2.2.1. Chemical Oxidation Experiment

We designed an experiment in which the different fossil standard samples (Table 1) were exposed to consecutive oxidative cleaning steps using a solution of sodium hypochlorite (corals), basic potassium persulfate (foraminifera and tooth enamel), and perchloric acid (diatoms), following the methods described in Section 2.3. The first oxidation step had the objective of removing any external (non-mineral-bound) organic material and is part of our standard cleaning procedure. The second oxidation step was used to evaluate the potential effect of exposure to strongly oxidizing conditions on the N content and isotopic composition of the remaining fossil-bound organic matter. If the mineral matrix provides an effective barrier against chemical attack, we would expect to see no change in N content or $\delta^{15}N$ when comparing the first and second oxidative cleanings. In contrast, if the matrix is permeable, the organic matter would be vulnerable to chemical attack, and we would expect a decrease in N content. In addition, if this process preferentially removes ^{14}N or ^{15}N, we would expect a change in $\delta^{15}N$ and a decrease in N content. In contrast, if the mineral matrix is permeable but organic material is removed without any isotopic discrimination, we would expect to find a decrease in N content but no change in $\delta^{15}N$.

2.2.2. Mineral Dissolution Experiment

Artificial dissolution experiments of the calcite (foraminifera), aragonite (corals), and enamel (teeth) standards were performed by adding different amounts of HCl to known quantities of the standard mineral powder. We tested three treatments that resulted in around 25%, 50%, and 70% dissolution in corals and foraminifera, and in around 40%, 60%, and 75%–90% dissolution in enamel. Each treatment was performed in triplicate for each standard fossil material. After dissolution, the remaining powder was rinsed five times with Milli-Q water and dried in a clean oven at 60°C. The dry powder was weighed and its N isotopic composition and N content were determined using the methods described in Section 2.3. We compared the results obtained when measuring the samples directly after dissolution to those obtained when the samples were recleaned after the dissolution treatment, in order to evaluate the possibility that organic matter was exposed during the dissolution but not removed during the rinsing with Milli-Q water.

For the diatom dissolution experiment, ~15–25 mg aliquots of cleaned diatom standard material were placed in pre-combusted 4 ml glass vials and filled with 4 ml 0.15 M NaOH solution. The vials were then placed in an 85°C water bath for ~15 min (~40% dissolution), ~1 hr (~60% dissolution), and 1.5 hr (70% dissolution). In the 70% dissolution experiment, the supernatant was replaced with fresh 0.15 M NaOH solution after 1 hr and the samples were placed back in 85°C water bath for another 0.5 hr. In all experiments, the supernatant was discarded after heating, and the residual opal samples were rinsed 5 times with Milli-Q water and dried in a clean oven at 60°C for 36 hr. N isotopic composition and N content were determined using the methods described in Section 2.3.

The aim of these experiments was to compare the potential effects of partial dissolution of the inorganic mineral matrix on the isotopic composition of fossil-bound organic matter. If the organic matter is uniformly distributed and is completely removed after dissolution, we would expect to see no change in N content or $\delta^{15}N$. In contrast, if the isotopic composition of the organic N within the fossil is heterogeneous and dissolution preferentially affects parts of the fossil with a distinct isotopic composition or N concentration, we would expect to see differences in $\delta^{15}N$ and/or N content between the different treatments and the untreated control sample. Likewise, if organic matter is exposed during dissolution, but not removed during washing, we could see an increase in N content. However, this additional N should be removed if the samples are oxidatively cleaned after dissolution. If there are no differences in $\delta^{15}N$ between the samples that are oxidatively cleaned after dissolution and the ones that are not, we could conclude that the exposure of organic matter does not alter its isotopic composition.

2.2.3. Thermal Degradation Experiment

We performed a series of laboratory experiments in which the cleaned diatom, coral, foraminifera and tooth enamel samples described in Table 1 were exposed to different temperatures (100°, 200°, 300°, 400°, and 500°C) in a muffle furnace for 24 hr. Aliquots of the different standard materials were placed in the muffle furnace inside 4 ml pre-combusted glass vials covered with pre-combusted aluminum foil. The muffle furnace was heated from room temperature to the target temperature in 1.5 hr and kept at temperature for 24 hr. Then, the furnace was allowed to cool down to a temperature below 50°C before the sample vials were taken out of the furnace. The N isotopic composition and N content of the remaining diatom, coral, foraminifera, and tooth enamel powder were measured following the procedure described in Section 2.3. Similar to the dissolution experiment described in the previous section, we compared the results obtained when measuring the samples directly after heating to those obtained when the samples were recleaned after the heating treatment.

The aim of these experiments was to compare the potential effects of thermal degradation of fossil-bound organic matter on its isotopic composition. If fossil-bound organic matter is not altered during heating, we would expect to see no change in N content or $\delta^{15}N$ with increasing temperature. However, if the thermal degradation of fossil-bound organic matter is incomplete and affects preferentially a fraction of organic matter with a specific isotopic composition, we would expect a change in both N content and isotopic composition. In contrast, if the fraction of fossil-bound organic matter that is affected by heating is completely combusted, we would expect to find a decrease in N content, but no substantial change in isotopic composition. Finally, if there are no differences in N content and $\delta^{15}N$ between the samples that are oxidatively cleaned after heating and the ones that are not, we could conclude that the exposed organic material is completely combusted.

2.3. Analysis of Fossil-Bound Nitrogen Isotopes

The analyses were performed in the laboratories of the Organic Isotope Geochemistry Group of the Department of Climate Geochemistry at the MPIC. The nitrogen isotopic composition (expressed as $\delta^{15}N = ((^{15}N/^{14}N)_{sample}/(^{15}N/^{14}N)_{air} - 1) *1000$) of the samples was determined using the oxidation-denitrifier method (Knapp et al., 2005). Prior to analysis, sample powders were chemically cleaned following standard reductive and oxidative cleaning steps that have been described previously for each fossil type (Leichliter et al., 2021; Ren et al., 2009; Studer et al., 2015; Wang et al., 2014, 2015), as described below.

The reductive cleaning step was the same for all fossil types. 50 mg of powdered fossil samples were weighed into 15 ml polypropylene centrifuge tubes, and 7 ml of sodium bicarbonate-buffered dithionite citrate solution (Mehra & Jackson, 1958) was added to the samples. The tubes were then placed in a 80°C water bath for 10 minutes. This step was originally included to remove metal oxide coatings, which could potentially trap exogenous nitrogen (Mehra & Jackson, 1958; Ren et al., 2009). After cooling, samples were centrifuged, the solution was decanted, and the remaining powder was rinsed three times with 10 ml of Milli-Q water (18.2 MΩ cm, <5 ppm TOC) and transferred to pre-combusted 4 ml glass vials.

Following our standard protocols, the oxidative cleaning was performed using re-crystalized potassium persulfate for foraminifera and enamel material, sodium hypochlorite for coral samples, and perchloric acid for diatom samples. In the first protocol, a basic potassium persulfate solution consisting of 2 g of sodium hydroxide, 2 g of potassium persulfate and 100 ml of Milli-Q water was added to the foraminifera and enamel samples, which were subsequently autoclaved for 65 min at 120°C. The oxidative solution was removed by aspiration after centrifugation, and the remaining powder was rinsed four times with 4 ml Milli-Q water and dried in a clean oven at 60°C for 24 hr. In the second protocol, coral samples were soaked in 4.25 ml sodium hypochlorite (10%–15% available chlorine), in pre-combusted glass vials placed horizontally on a shaker table rotating at 120 rpm for 24 hr. Samples were then centrifuged, the solution was removed by aspiration, and the remaining powder was rinsed three times with Milli-Q water and dried in a clean oven at 60°C for 24 hr. In the third protocol, diatoms were cleaned with 7% perchloric acid in a boiling water bath for 1 hr in 15 ml polypropylene centrifuge tubes, centrifuged and decanted. The remaining powder was transferred to pre-combusted 40 ml glass tubes and subsequently cleaned with 60% perchloric acid in boiling water bath for 2 hr, rinsed with Milli-Q water until the pH was neutral, and dried for 24–48 hr in a clean oven at 60°C.

After cleaning, foraminifera, coral and enamel powder were demineralized using 4 *N* hydrochloric acid, and organic N was oxidized to nitrate with a solution prepared using 0.7 g recrystallized potassium persulfate, 4 ml of

6.25 N NaOH, and 95 ml Milli-Q water. Samples were autoclaved for 65 min at 120°C, and centrifuged. Cleaned diatoms were dissolved and the organic N released from the frustules oxidized to nitrate in one step by adding 1 ml of a solution prepared using 3 g of recrystallized potassium persulfate, 12 ml of 6.25 N NaOH, and 83 ml Milli-Q water. Diatom samples were autoclaved at 120°C for 95 min. For all fossil types analyzed, the concentration of nitrate in the oxidized solutions was determined by chemiluminescence (Braman & Hendrix, 2002). An aliquot of the nitrate solution equivalent to 5 nmol of N was quantitatively converted to nitrous oxide (N_2O) using the denitrifier method (Sigman et al., 2001), and the $\delta^{15}N$ of the N_2O generated was determined by a purpose-built inlet system coupled to a Thermo MAT253 Plus stable isotope ratio mass spectrometer (Weigand et al., 2016).

International reference nitrate standards (USGS34, IAEA-NO-3) were analyzed with each batch of samples and used to calculate N concentration and calibrate the isotopic composition of samples versus air N_2. The N content and $\delta^{15}N$ of the persulfate oxidation reaction blank was measured in duplicate in each batch of samples and was used to correct the fossil-bound measurements. International reference amino acid standards (USGS40 and USGS41 or USGS65) were analyzed to monitor the persulfate oxidation. The N content of the blank across the different batches was between 0.1 and 0.4 nmol/ml. The precision (1σ) for repeated $\delta^{15}N$ measurements of the control standards described in Section 2.1 was 0.10‰ for the MF-1 foraminifera standard ($n = 9$), 0.16‰ for the MF-2 standard ($n = 9$), 0.10‰ for the LO-1 coral standard ($n = 9$), 0.17‰ for the PO-1 coral standard ($n = 9$), 0.11‰ for the AG-Lox tooth standard ($n = 6$), 0.28‰ for the Noto-2 tooth standard ($n = 3$), 0.68‰ for the Hippo-1 standard ($n = 3$), and 0.02‰ for the DI-1 diatom standard ($n = 3$).

2.4. Statistical Analysis

The results of the multiple measurements for each treatment in the different experiments are presented as means ± 1 standard deviation. When calculating the difference between the control and the treatment, the standard deviations of the two measurements were propagated. The mean $\delta^{15}N$ values obtained after the different treatments were compared to those obtained for the untreated control sample with a Student's t-test. A p-value of <0.01 was considered statistically significant in the discussion, p-values are reported in the Supporting Information.

3. Results and Discussion

3.1. Impact of Chemical Oxidation on Fossil-Bound $\delta^{15}N$ and N Content

Relative to the uncleaned sample, our experiments showed a significant decrease in N content during the first oxidative cleaning in all the fossils analyzed, except in the diatom sample (Figure 2a). The N content of the uncleaned samples was 103% higher than after the first oxidative cleaning (i.e., the control sample) for the North Atlantic mixed foraminifera sample, 250% higher for the Southern Ocean mixed foraminifera sample, 331% higher for the deep-sea coral, 46% higher for the shallow water coral, 309% higher for the modern elephant enamel sample, 305% higher for the fossil hippo enamel sample and 417% higher for the fossil suid enamel sample (Figure 2c). The N content of the uncleaned diatom sample was only 7% higher than after the first oxidative cleaning, and not statistically significant. The large reduction observed in most fossil types after the first cleaning was the expected result, because the purpose of this first cleaning step was to remove external (non-mineral-bound) organic matter from the sample. The external organic matter was likely mostly from the natural (e.g., sedimentary) environment in most cases, but some of it may have derived from contamination during collection and storage.

Not surprisingly, the removal of the external organic N was associated with variable changes in the isotopic composition of the different fossil types (Figure 2b). The $\delta^{15}N$ of the North Atlantic mixed foraminifera sample increased significantly by 1.25 ± 0.16‰, but the $\delta^{15}N$ of the Southern Ocean mixed foraminifera sample decreased significantly by 0.87 ± 0.23‰ (Figure 2d). The $\delta^{15}N$ of the deep-sea coral increased significantly (by 0.67 ± 0.11‰), while the shallow water coral $\delta^{15}N$ barely changed (decreasing by 0.06 ± 0.19‰, but not significantly), despite the substantial decrease in its N content. The $\delta^{15}N$ change of the diatom sample (from 0.93 ± 1.21‰ to 1.78 ± 0.02‰) was not significant, but cleaning resulted in a strong decrease in standard deviation. Suid and hippo fossil enamel showed large increases (2.99 ± 0.40‰ and 4.21 ± 1.30‰, respectively), but modern enamel did not show a significant change (decreasing by 0.22 ± 0.15‰), despite the large reduction in its N content. The absence of significant $\delta^{15}N$ changes in the modern enamel sample and the modern shallow-water coral core sample suggest that most of the organic matter present in the drilled tooth enamel material and
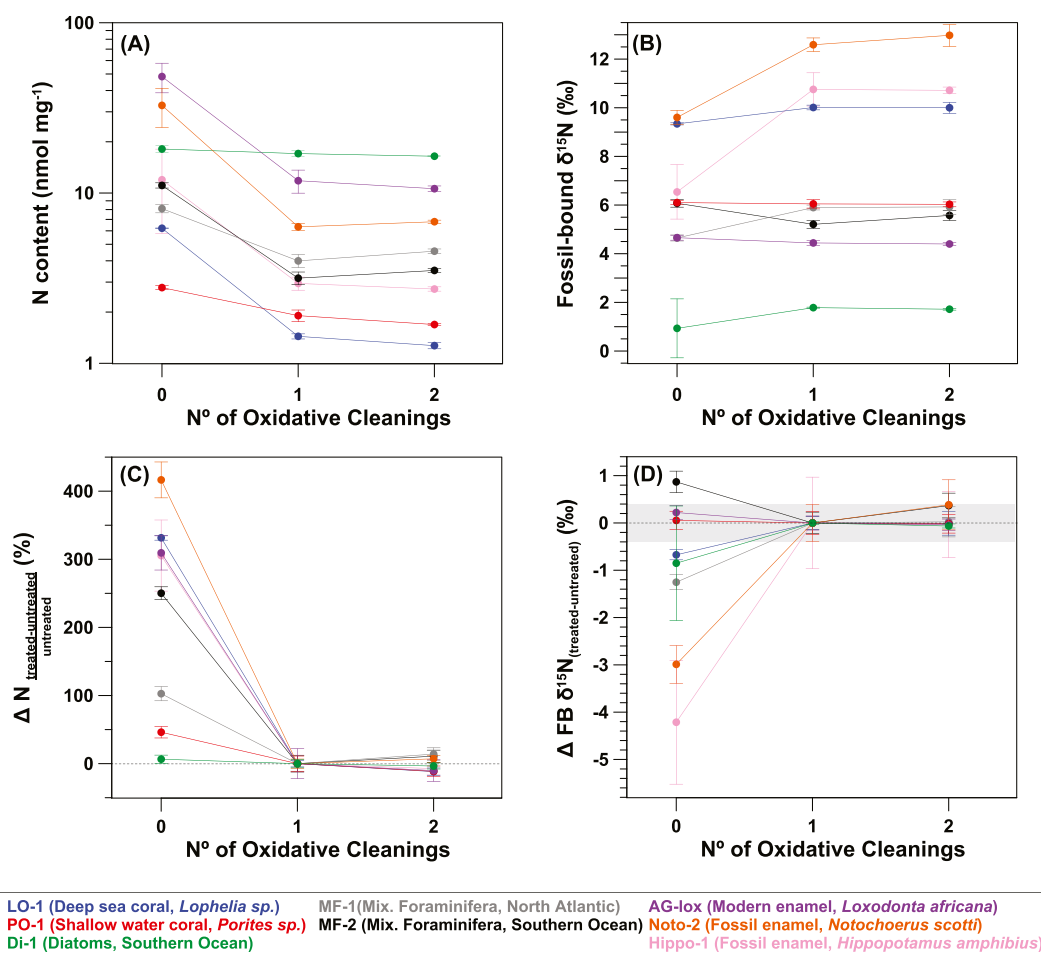
Figure 2. Evaluation of the effect of exposure to strongly oxidizing conditions on fossil-bound δ^{15}N. Effect of consecutive oxidative cleanings with solutions of sodium hypochlorite (corals), potassium peroxodisulphate (foraminifera and teeth) and perchloric acid (diatoms) on fossil-bound (a) N content and (b) δ^{15}N. In (a), a $\log_{10}$ scale is used for the Y axis to facilitate comparison of the different fossil types. (c) Percent N content difference of 0 oxidations and 2 oxidations with respect to the 1 oxidation treatment. (d) Same difference as in (c) but for δ^{15}N instead of percent N content. The gray shaded area highlights differences between the treated and untreated samples that are within $\pm0.4‰$, that is, within two standard deviations of the average analytical precision observed for the control samples (see Section 2.3). In (a) and (b), error bars represent the 1 sigma standard deviation of triplicate oxidation experiments performed for each treatment (see Figure 1). In c and d, error bars indicate the propagated uncertainty from a and b, respectively. Note that the control sample in this experiment is the sample that has been cleaned once, not the uncleaned sample.

coral core was endogenous to the organism and well-preserved despite not being bound to the mineral matrix. However, the significant δ^{15}N change associated with the removal of external organic material in other relatively recent (i.e., Holocene) samples (e.g., deep-sea coral and the two foraminifera samples) and the very large change associated with the Plio-Pleistocene fossil enamel samples highlight the potential for isotopically distinct N to become associated with fossil surfaces and thus the need for harsh cleaning prior to the analysis of the N isotopic composition of fossil bound organic material. Whether δ^{15}N increased or decreased upon cleaning could depend on multiple factors, some of which may be identifiable. For example, foraminifera and diatoms derive from deep sea sediments, and sedimentary organic N is known to undergo a diagenetic increase in δ^{15}N (Freudenthal et al., 2001; Robinson et al., 2012), such that cleaning might be expected to lower the δ^{15}N of the remaining N (i.e., the fossil-bound N). However, there is a range of possible influences on the δ^{15}N of the external N, which vary with sample type and sample origin. In addition, sample handling prior to analysis (e.g., drilling of coral and enamel samples and washing, sieving and separation of foraminifera and diatom samples) can introduce N contamination. Thus, the reasons for the observed δ^{15}N changes upon cleaning (e.g., as to whether δ^{15}N increases or decreases) are not pursued further here.

Notably, the subsequent re-oxidation of all the samples analyzed resulted in negligible changes in N content and isotopic composition (Figures 2a and 2b). In fact, for all fossil types analyzed, the N content and $\delta^{15}N$ of the re-oxidized samples were statistically indistinguishable from those obtained after a single oxidation (Figures 2c and 2d). These results show that the mineral matrix indeed represents an effective physical barrier that protects organic matter against chemical attack, even with exceptionally strong oxidizing solutions.

Our findings are in good agreement with previous experiments designed to optimize the cleaning protocols of different fossil types (e.g., foraminifera, corals, tooth enamel, otoliths or diatoms) using either sodium hypochlorite or perchloric acid. In these experiments, the different fossil types were exposed to the oxidizing solutions for different times, either at room temperature or with moderate heating to 60–70°C (Kast, 2020; Lueders-Dumont et al., 2018; Ren, 2010; Sigman et al., 1999). In general, all the studies showed a drop in N content and changes in $\delta^{15}N$ after a few hours of exposure to the reagent, as expected from the removal of the external (non-bound) organic matter. However, the N content and $\delta^{15}N$ of the sample stabilized with time, so that any additional time exposure to the reagent did not change N content or isotopic composition. In general, the application of heat resulted in a faster removal of the external organic matter, but did not change the N content or the $\delta^{15}N$ of the fossils analyzed with respect to that of the samples oxidized at room temperature. The original aim of these studies was to identify the optimal time and chemical reagent for the complete removal of external organic matter, but they also provided strong support for the stability of fossil-bound material.

In previous work, one exception to these uniformly straightforward findings has involved the cleaning of diatom frustules. Very fresh diatom opal, such as from diatom cultures, appears to be vulnerable to specific reagents, such as hydrogen peroxide (Morales et al., 2013). However, diatom opal is rapidly altered in the marine environment, for example, increasing its aluminum content by more than 10 times upon incorporation in the sediments (Ren et al., 2013). This alteration appears to "harden" the mineral to render it robust against hydrogen peroxide. Still, for Holocene opal oozes from the North Pacific, there are signs that diatom microfossils might not be able to protect fossil-native N against boiling perchloric acid (Brunelle et al., 2007). As described below, the heating experiments from the current study may explain these earlier results.

Previous work also suggests that, for diatom opal, some oxidative reagents and treatments can be too weak to fully remove externally vulnerable N, which required extensive testing to settle on the current cleaning protocol (Brunelle et al., 2007; Robinson et al., 2004). In contrast, for carbonate and phosphate biominerals, reagent choices (e.g., persulfate *vs.* hypochlorite) have shown little to no influence (Kast, 2020; Leichliter et al., 2021; Lueders-Dumont et al., 2018; Ren et al., 2009; Straub, 2012; Wang et al., 2015), albeit with a recrystallization-related exception for the otoliths of one fish species (Lueders-Dumont et al., 2018). We suspect that this difference of diatom opal from calcium carbonate and phosphate minerals relates to the unique and mutable characteristics of diatom opal, as will be discussed further in the context of the heating experiments in Section 3.3.

Our oxidant exposure experiments were, of course, not conducted on the geologic time scale, that is, over thousands to millions of years. In this and other regards, the experiments are not an ideal simulation of the exposure of fossil material to sedimentary diagenesis. However, the oxidants used were far more aggressive than those used by microbes to attack sedimentary organic matter. Thus, our findings are strongly supportive of the view that fossil-bound N is well protected by the mineral matrix from the external environment, supporting the argument that fossil-bound N preserves the $\delta^{15}N$ of fossil-native organic matter generated by ancient organisms.

3.2. Impact of Biomineral Dissolution on Fossil-Bound $\delta^{15}N$ and N Content

In our first set of experiments, samples were measured directly after the dissolution treatment (left panels in Figure 3). The results of these experiments showed a progressive increase in N content per mg of mineral as we increased the percentage of dissolved mineral matrix (Figures 3a and 3c). The proportional N content increase found in the most aggressive treatment was similar for foraminifera (20%–34%) and corals (21%–22%), slightly higher for tooth enamel (32%–42%) samples, and substantially lower for diatoms (2%) (Figure 3c). The observed N content increase from the most aggressive treatment was statistically significant compared to the untreated sample for all the fossil types, except for the diatom sample.

The observed increase in N content during dissolution could indicate that: (a) organic matter exposed during the dissolution experiment was not completely removed by rinsing multiple times with Milli-Q water, or (b) dissolution preferentially occurred in N-poor parts of the mineral matrixes. In order to distinguish between these two
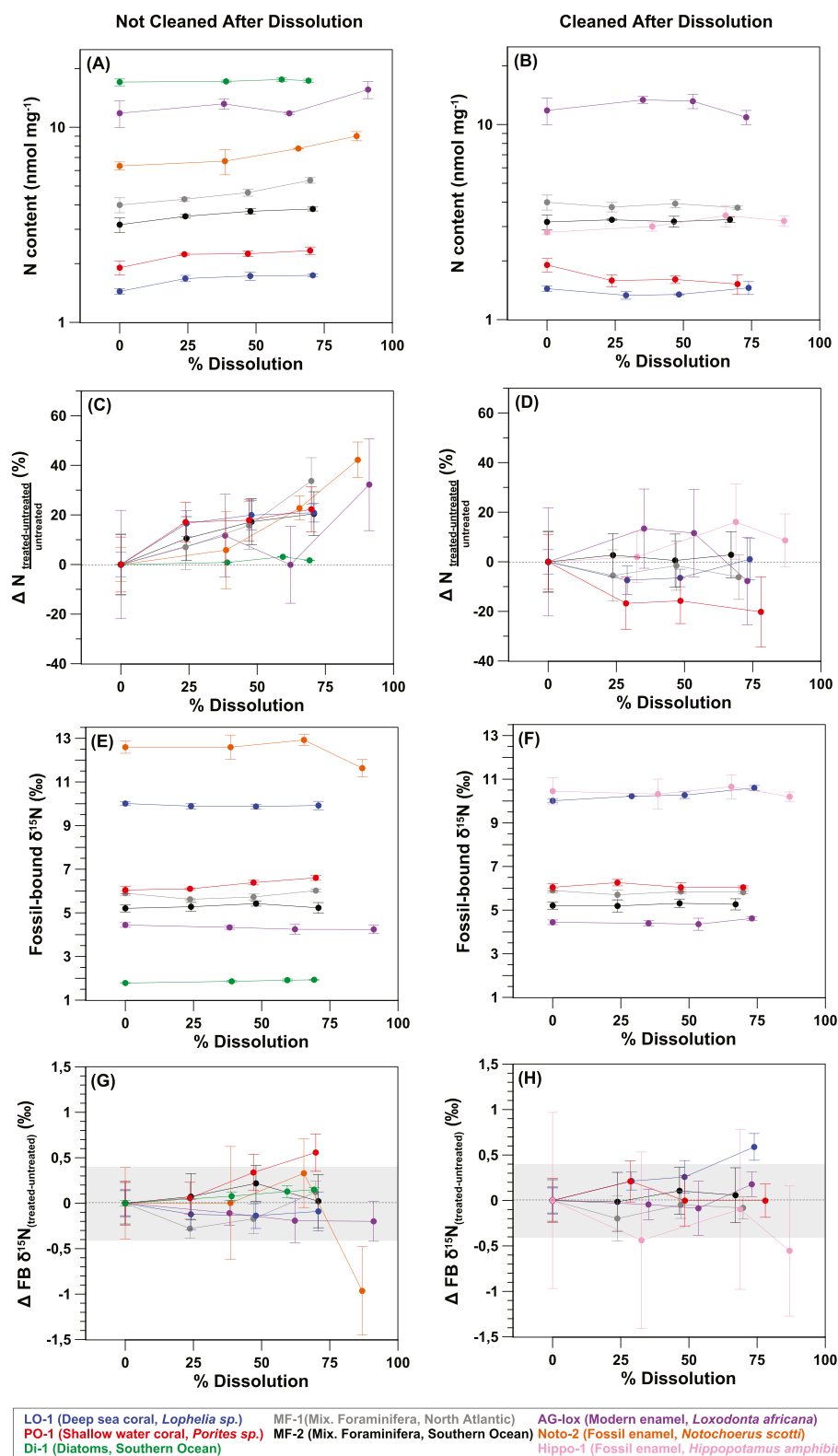
Figure 3.

possibilities, we repeated the dissolution experiment but introduced a second oxidative cleaning step after the dissolution treatment (right panels in Figure 3). If the increase in N content was caused by incomplete removal of organic matter exposed during dissolution, we would expect that this organic matter would be removed during this additional oxidative cleaning. However, if it was caused by dissolution of N-poor regions of the fossils, we would expect that the increasing N content trend would persist after the additional cleaning. Our results show that after the second cleaning, for all of the fossils except for the shallow water coral, the N content of the fossils analyzed after the different dissolution treatments was statistically indistinguishable from the untreated control sample. These results clearly indicate that the N increase observed in the first experiment for most of the fossil types was due to incomplete removal of organic matter that was exposed during the dissolution treatment; and, consequently, they confirm that the dissolution did not have a significant preference for N-rich or N-poor biomineral.

In contrast, for the shallow water coral, there was a similar decrease (of 16%–20%) during all dissolution treatments relative to the undissolved sample. For this sample, an argument can be made that the first dissolution (of ~25%) did access N-rich skeletal material. The decline in N content was relatively constant with respect to the fraction dissolved, which may indicate the dissolution of a discrete N-rich biomineral component, as opposed to dissolution being guided by a continuous range in biomineral N content. Scleractinian coral skeleton is observed to contain microcrystalline septa that are associated with the onset of calcification (the "rapid accretion deposits," also referred to as "centers of calcification"), representing ~5% of the skeleton (Stolarski, 2003). Spatially resolved measurements indicate that the rapid accretion deposits are microcrystalline and richer in organics as well as non-calcium cations than the "thickening deposits," the main skeletal component (Cuif & Dauphin, 2005). There is also evidence that the rapid accretion deposits are the first component to undergo diagenesis and recrystallization (Frankowiak et al., 2013). Thus, there are both conceptual and observational expectations that this material would be particularly vulnerable to acid dissolution. Accordingly, the 16%–20% decline in N content of the coral sample under any level of acid addition in our experiments may reflect the nearly complete dissolution of this microcrystalline component. However, the observed changes in N content were relatively small, and deep-sea corals did not show a clear N content decrease, especially in the 74% dissolution experiment. Thus, this possible role for rapid accretion deposits remains to be confirmed by future experiments.

Despite the differences in N content found in most fossil types between our two versions of the dissolution experiment (i.e., with and without subsequent oxidative cleaning), the effect of partial dissolution on $\delta^{15}N$ was minimal in both cases (Figures 3e–3h). In most of the fossils, the difference between the acid treatments and the untreated samples was within 0.4‰ (Figures 3g and 3h), which is within two standard deviations of the average analytical precision observed for the control standards (see Section 2.3).

We first consider the implications of the second experiment (with subsequent oxidative cleaning), which is the better analog for actual samples. In this experiment, the lack of change in dissolved relative to undissolved samples indicates that the dissolution did not preferentially remove isotopically distinct N. This is not surprising. For isotopic change to have occurred, there would need to be both (a) distinct solubilities among components of the biomineral and (b) isotopic differences that correlate with the susceptibility to dissolution. Our results show very little change in N content, already arguing that N content variations, if they occur at all, are not strongly correlated with biomineral variation. Otherwise, the comparison of our two experiments confirm that any N exposed by the dissolution process is successfully removed by our fossil cleaning.

Turning to the first experiment (i.e., without subsequent oxidative cleaning), beyond the conclusions stated above, the N content increases indicate that a portion of the N exposed during dissolution has an adequately robust structural (biochemical) framework to remain attached at the biomineral surface during repeated rinsing of the sample with Milli-Q water. However, the $\delta^{15}N$ results indicate that this now-superficial N was not greatly changed in $\delta^{15}N$ by the dissolution process. This, again, is not surprising. Peptide bond hydrolysis could induce

Figure 3. Evaluation of the effect of biomineral dissolution on fossil-bound $\delta^{15}N$. Left panels (a, c, e, and g) show results for samples measured directly after the dissolution treatment. Right panels (b, d, f, and h) show results for samples that were subjected to an additional oxidative cleaning after the dissolution treatment. (a, b) N content and (e, f) $\delta^{15}N$ of different fossil types. In (a) and (b), a $\log_{10}$ scale is used for the Y axis to facilitate comparison of the different fossil types. (c, d) Percent N content difference between each dissolution treatment and the untreated sample. (g, h) $\delta^{15}N$ difference between each dissolution treatment and the untreated sample. The gray shaded area highlights differences between the treated and untreated samples that are within ±0.4‰, that is, within two standard deviations of the average analytical precision observed for the control samples (see Section 2.3). In a, b, e, and f, error bars represent the 1 sigma standard deviation of triplicate dissolution experiments performed for each treatment (see Figure 1). In c, d, g, and h, error bars indicate the propagated uncertainty from a, b, e, and f, respectively.

significant isotopic fractionation (Bada et al., 1989). However, protein hydrolysis requires much higher acid/base concentrations and temperatures as well as longer reaction times (Roach & Gehrke, 1970). Accordingly, in our experiments, some N could be exhumed and survive the dissolution on the mineral surface, without undergoing clear isotopic changes in the process. Most of the data are consistent with this scenario.

We now turn to the few isotopic changes that were observed. In our first experiment (i.e., without subsequent oxidative cleaning), the biggest difference in $\delta^{15}N$ with respect to the untreated samples ($-0.96 \pm 0.49‰$) was observed after the 87% dissolution treatment of one of our fossil enamel samples (Figures 3e and 3g). This treatment also resulted in one of the largest increases in N content (42%) with respect to the untreated sample. However, due to the relatively large standard deviation in $\delta^{15}N$ obtained for replicate analysis of the fossil, this difference was not statistically significant ($p = 0.03$). The large standard deviation obtained for the untreated sample, and across the different treatments, suggests a more heterogeneous isotopic composition for this particular fossil. Interestingly, in the case of the modern enamel sample, dissolution treatments up to 91% resulted in negligible changes in $\delta^{15}N$ values ($p = 0.08$), despite the large increase in N content (32%) relative to the untreated sample. The diatom sample showed one of the lowest changes in $\delta^{15}N$ ($0.15 \pm 0.03‰$) during the most aggressive treatment (69% dissolution). Paradoxically, this difference was statistically significant with respect to the untreated sample due to the extremely low standard deviation of the diatom replicate measurements. The only other sample that showed a statistically significant difference ($0.56 \pm 0.21‰$) was the shallow water coral sample when dissolved by 47%–70%. The differences observed in all the other coral, foraminifera and tooth fossils were statistically indistinguishable from the untreated samples.

In our second experiment (i.e., with subsequent oxidative cleaning), the difference between the different dissolution treatments and the untreated samples were even smaller (Figures 3f and 3h). In contrast to the first experiment, the shallow-water coral sample was undistinguishable from the control sample in all the treatments. However, the deep-water coral sample showed a statistically significant difference with respect to the untreated sample. Unfortunately, we could not perform the second experiment for the suid fossil enamel sample nor for the diatom sample because no sample powder was left. Nevertheless, the rest of the fossil samples analyzed, including an additional Plio-Pleistocene fossil enamel sample, were indistinguishable from the untreated samples (Figures 3f and 3h). We consider this second experiment more directly comparable to environmental samples that were exposed to dissolution in the past, because any fossil-native organic matter that might have been exposed during dissolution would be removed by our standard cleaning protocol and not measured.

The fact that the $\delta^{15}N$ of the diatom exposed to ~70% dissolution and the deep-sea coral samples were statistically different from the untreated sample is not particularly concerning for the application of the fossil-bound $\delta^{15}N$ method. The diatom samples were isolated from deep-sea sediment cores. Thus, they have already undergone substantial dissolution in the water column and sediments as part of normal diagenetic processes (Van Cappellen et al., 2002). The ~70% further dissolution would thus represent an extreme degree of dissolution relative to the starting diatom opal material. Despite this situation, the observed $\delta^{15}N$ changes were very small ($0.15 \pm 0.03‰$) and would not significantly impact the paleoceanographic interpretation. The deep-sea coral $\delta^{15}N$ increase (of $0.59 \pm 0.15‰$) at 75% dissolution applied only to the dissolution experiment that included subsequent cleaning (Figures 3h vs. 3g), which raises questions about its robustness. On the other hand, deep-sea corals record extensive periods of time and can capture major $\delta^{15}N$ changes (Wang et al., 2014), so the sample might be more heterogeneous and thus vulnerable to preferential loss of isotopically distinct material.

In summary, the stability of $\delta^{15}N$ after the different dissolution treatments indicate a generally uniform isotopic composition for foraminifera-, coral-, enamel-, and diatom-bound organic material, and imply that the N exposed during dissolution is lost without significant isotopic discrimination. This conclusion is also supported by the similarity in the isotopic composition observed in our two experiments (with/without subsequent oxidative cleaning) despite significant differences in N content (Figures 3g and 3h). More practically, the second experiment indicates that the partial dissolution of fossil opal, calcite, aragonite or enamel matrixes has a negligible effect on the N content and N isotopic composition of fossil-bound organic matter. These results are consistent with those obtained in a foraminifera $\delta^{15}N$ ground-truthing field study near Bermuda, which suggest that foraminifera-bound N loss during early seafloor diagenesis does not occur with significant isotope fractionation because any newly exposed N is completely lost rather than isotopically altered (Smart et al., 2018).

In addition, our dissolution experiment results provide a framework for understanding the effect of calcite recrystallization in marine sediments. A remarkable finding from the study of early Cenozoic planktonic foraminifera-bound $\delta^{15}N$ is that the fossil-bound N content and $\delta^{15}N$ are preserved (Kast et al., 2019) despite the evidence for substantial recrystallization and isotopic resetting of the foraminifer tests in deep sea sediments (Killingley, 1983; Pearson et al., 2001, 2007). Our results indicate that the organic matter exposed by acid dissolution, at least in part, remains physicochemically connected with the surface of the remaining biomineral. Considering that the dissolution–reprecipitation of foraminiferal calcite is fast and occurs at a small spatial scale (Chanda et al., 2019), we hypothesize that the "exposed" organic N could be re-encapsulated in the recrystallized biomineral before it is lost or altered by bacterial attack.

3.3. Impact of Thermal Decomposition on Fossil-Bound $\delta^{15}N$ and N Content

As with the dissolution experiments, in our first set of thermal degradation experiments samples were measured directly after the heating treatment, without a subsequent oxidative recleaning (left panels in Figure 4). Our results showed no significant change in N content for all fossil types at 100° and 200°C, except for diatoms (Figures 4a and 4c). At temperatures >200°C, deep and shallow water aragonitic coral samples showed a progressive decrease in N content of 12% and 42%, respectively, at 300°C, 49% and 59% at 400°C, and 80% and 79% at 500°C. In contrast, the two calcitic mixed foraminifera samples showed no significant N losses at 300°C, only a moderate decreased at 400°C (15% and 27%), and a large decline at 500°C (80% and 82%). Interestingly, at 400°C, the decline observed in the foraminifera was substantially smaller than the one found in the corals, but, at 500°C, N losses were comparable for both fossil types. Finally, the N content of the modern and fossil enamel samples was statistically indistinguishable from that of the untreated samples up to 400°C, and decreased by only 33% at 500°C in the fossil sample, while there was not statistically significant N loss from the modern enamel sample. Thus, tooth enamel is an interesting contrast with the ~80% reduction in calcitic foraminifera and aragonitic corals. These results indicate that the fraction of N lost at different temperatures depends on the mineral composition and structure of the fossil.

The effect of the different thermal treatments on the isotopic composition of fossil-bound N also varied widely across the different fossil types analyzed (Figures 4e and 4g). All fossils, except the diatoms, showed negligible changes in $\delta^{15}N$ at 100°C. At 200°C, deep-sea corals increased with respect to the untreated samples by 0.52 ± 0.17‰, and the two foraminifera samples by 0.41 ± 015‰ and 0.75 ± 0.18‰, respectively, but the shallow water corals and the tooth enamel samples showed no significant changes (Figure 4g). At 300°C, deep-sea and shallow water coral $\delta^{15}N$ increased moderately by 1.10 ± 0.20‰ and 0.75 ± 0.19‰, respectively. In contrast, the $\delta^{15}N$ increase observed in the two foraminifera samples (0.62 ± 0.14‰ and 0.75 ± 0.25‰) was indistinguishable from the one observed at 200°C, while the two tooth enamel samples continued to show no significant change. At 400°C, the $\delta^{15}N$ increases observed for the deep and shallow corals (1.12 ± 0.24‰ and 0.74 ± 0.30‰) and for the two foraminifera samples (0.67 ± 0.16‰ and 0.95 ± 0.16‰) were indistinguishable from those observed at 300°C. Again, the two tooth enamel samples did not show any significant $\delta^{15}N$ change. Finally, at 500°C, the $\delta^{15}N$ increase of the deep-sea coral (1.83 ± 0.37‰) and the two foraminifera samples (3.19 ± 0.32‰ and 3.57 ± 0.49‰) was significantly higher than in the experiment performed at 400°C, and coincided with substantial N loss, of about 80%. However, the $\delta^{15}N$ of the shallow water coral dropped to values similar to those found in the untreated sample, despite a similar N loss. As in the previous treatments, the two tooth enamel samples did not show any significant change at 500°C. Thus, our results reveal that both the N loss and the degree of isotopic change at different temperatures is directly linked to the mineral composition of the fossil.

In order to investigate further the relationship between N loss and $\delta^{15}N$ changes, we estimate the isotope effect of thermal loss of fossil bound N. The isotope effect (ε) expresses the degree of isotopic discrimination and is commonly defined as the ratio of reaction rates at which the two isotopes are converted from reactant to product (i.e., ε (‰) $= ((1 - {}^{15}k/{}^{14}k) \times 1000)$; where ${}^{x}k$ is the rate constant for the ^{x}N-containing reactant). We use the slope of the correlation of $\delta^{15}N$ against the natural logarithm of the N content to obtain a Rayleigh model-based estimate of the net isotope effect associated with the loss of N caused by thermal decomposition (upper panels in Figure 5) (e.g., Fripiat et al. (2019). If we plot our results across the entire temperature range, i.e., from room temperature (RT) to 500°C, we obtain a significant correlation for the two foraminifera samples and deep-sea coral, but not for the shallow water coral and the tooth enamel samples (Figure 5a). However, the correlation for the shallow water coral sample was significantly improved if the 500°C treatment was excluded (Figure 5b). From
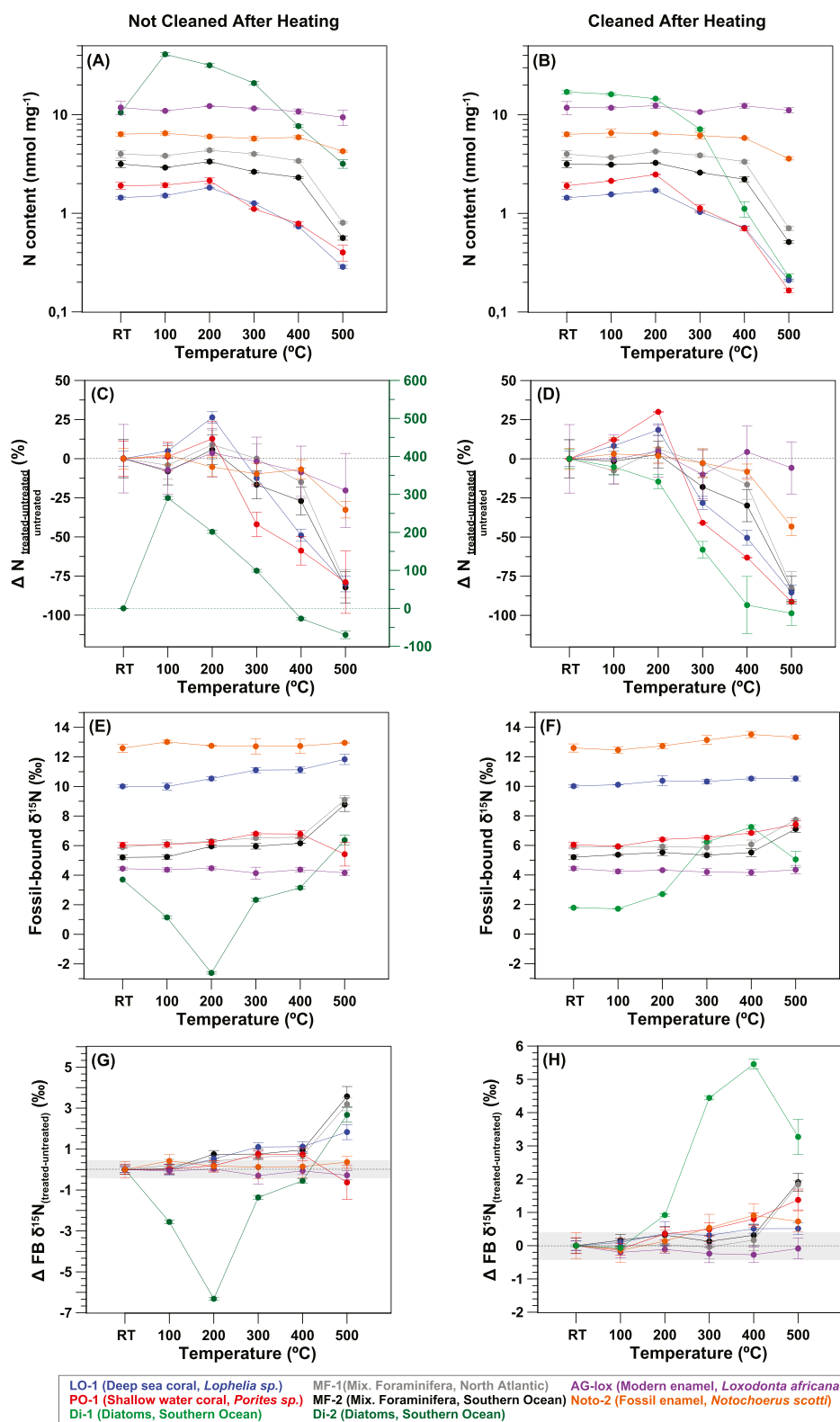
Not Cleaned After Heating | **Cleaned After Heating**

LO-1 (Deep sea coral, *Lophelia sp.*)   MF-1(Mix. Foraminifera, North Atlantic)   AG-lox (Modern enamel, *Loxodonta africana*)
PO-1 (Shallow water coral, *Porites sp.*)   MF-2 (Mix. Foraminifera, Southern Ocean)   Noto-2 (Fossil enamel, *Notochoerus scotti*)
Di-1 (Diatoms, Southern Ocean)   Di-2 (Diatoms, Southern Ocean)
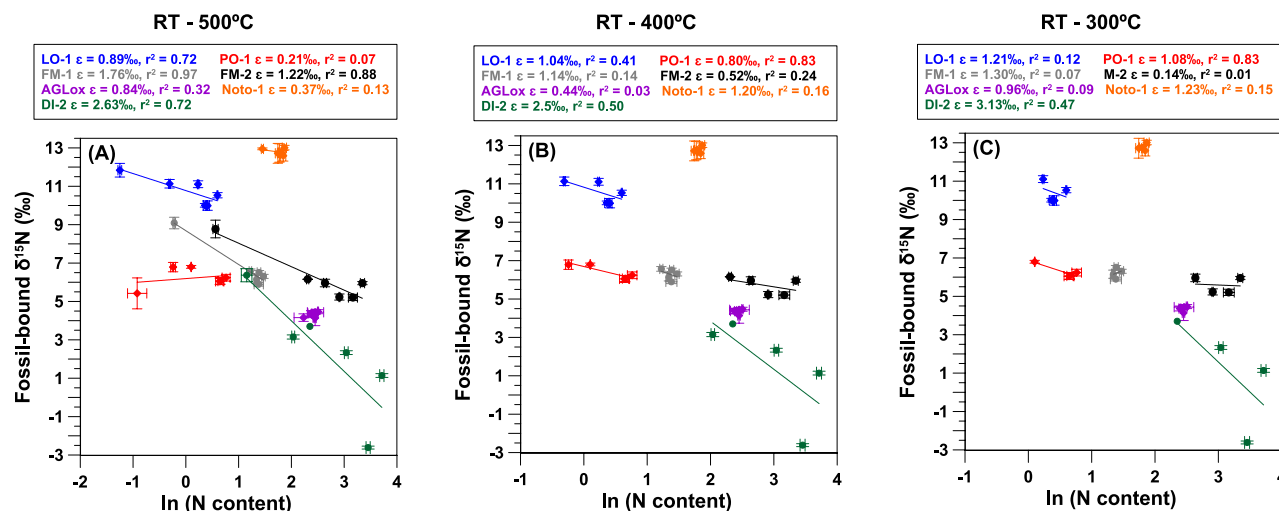
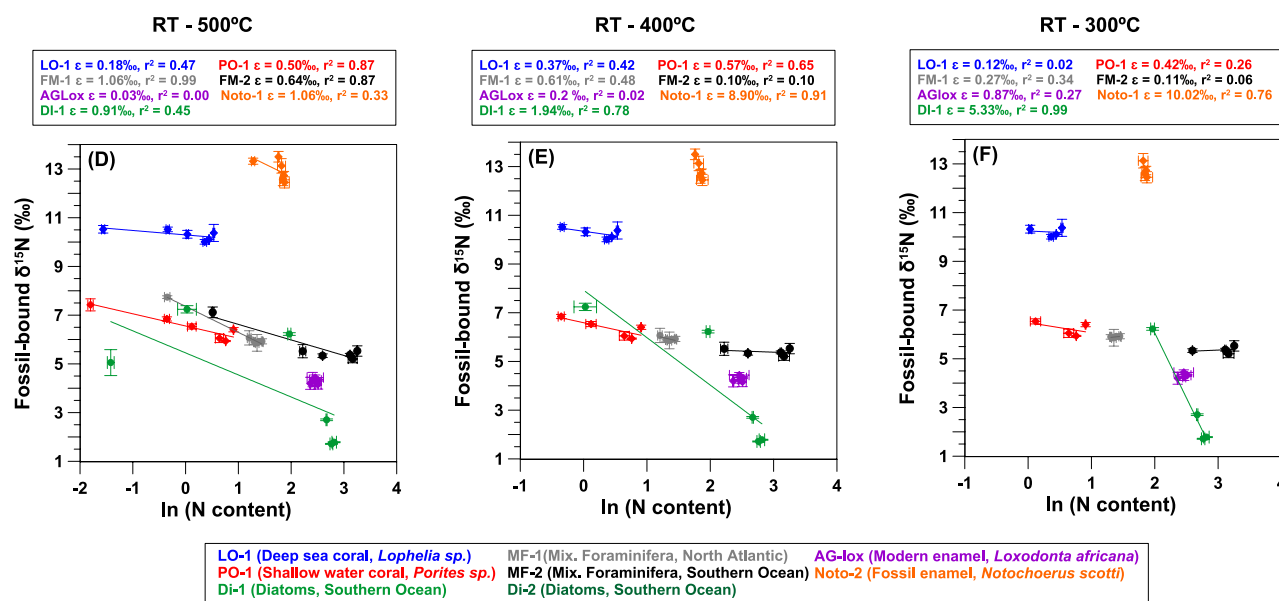**Figure 4.**

Figure 5. Evaluation of the isotope effect associated with thermal loss of fossil-bound N. Upper panels (a, b, c) show results for samples measured directly after the heating treatment. Lower panels (d, e, f) show results for samples that were subjected to an additional oxidative cleaning after the heating treatment. The figure shows fossil-bound δ15N *versus* the natural logarithm (ln) of the N content for the different temperature treatments shown in Figure 4. (a) Considering data from the entire temperature range from room temperature (RT), that is, our control sample, to 500°C, (b) from RT to 400°C, and (c) from RT to 300°C. The slope of the linear regressions (indicated above each plot) provides an estimate of the isotope effect (ε) associated with the loss of N from the fossil (see text). Error bars represent the 1 sigma standard deviation of triplicate experiments performed for each treatment.

Figure 4. Evaluation of the effect of heating on fossil-bound δ15N. Left panels (a, c, e, and g) show results for samples measured directly after the heating treatment. Right panels (b, d, f, and h) show results for samples that were subjected to an additional oxidative cleaning after the heating treatment. (a, b) N content and (e, f) δ15N of different fossil types. In (a) and (b) a log10 scale is used for the Y axis to facilitate comparison of the different fossil types. (c, d) Percent N content difference between each heating treatment and the control sample, that is, room temperature (RT). In c, percent N content values for the DI-2 sample are plotted against the right axis. (g, h) δ15N difference between each heating treatment and the control sample. The gray shaded area highlights differences between the treated and untreated samples that are within ±0.4‰, that is, within two standard deviations of the average analytical precision observed for the control samples (see Section 2.3). In a, b, e and f, error bars represent the 1 sigma standard deviation of triplicate heating experiments performed for each treatment (see Figure 1). In c, d, g, and h, error bars indicate the propagated uncertainty from a, b, e and f, respectively.

RT to 400°C, the correlation for the deep-sea coral sample was still significant, but it was not for the foraminifera samples. From RT to 300°C, the correlation was only significant for the shallow water coral sample. Interestingly, the estimated isotope effects for the two coral samples were relatively similar (ranging from 0.80‰ to 1.04‰) from RT to 500° and to 400°C, suggesting that the isotopic discrimination during thermal degradation was relatively similar at different temperatures for aragonitic samples. The isotope effects from the two foraminifera samples were also very similar to one another (1.76‰ and 1.22‰), suggesting a slightly higher isotope effect for calcite than for aragonite. Finally, as expected from the lack of variability in N content and $\delta^{15}N$, the correlation for the two tooth enamel samples was not significant across any of the temperature ranges analyzed. Thus, our results raise the possibility that the isotope effects during thermal degradation of fossil bound organic matter are different for aragonite, calcite and apatite samples.

As an alternative possibility, there may be isotopically distinct forms of N that are preferentially lost and retained that could explain or contribute to isotopic changes. In this case, the similar isotope effects observed for different biominerals could relate more to the organisms producing the fossil-bound N rather than the biomineral itself. Our strongest argument against this alternative interpretation is that nearly all regressions yield a weak negative (or insignificant) slope, which would seem unlikely if the isotopic changes were driven by preferential loss of specific N forms generated by different organisms.

During this first set of experiments, the behavior of the diatom sample was not consistent with the rest of the fossils and/or with expectations from thermal degradation of frustule bound organic matter. Our results showed substantial increases in N content (~300%) at 100°C relative to the untreated sample, suggesting substantial contamination of the frustule material with exogenous N (Figures 4a and 4c). This N content increase was accompanied by a significant reduction in $\delta^{15}N$ values (of 2.56‰) (Figures 4e and 4g). This contamination problem persisted at higher temperatures, and the N content of the treated samples at 200° and 300°C was also higher (and the $\delta^{15}N$ significantly lower) than that of the untreated control sample. A mass balance of the N change between the control sample and the 100°C measurements reveals that the $\delta^{15}N$ of the N added was 0.28‰. The ability of diatom opal to adsorb N species has been noted previously (Robinson et al., 2004), and it also appears to apply to carbon species (Zheng et al., 2002). We have not as yet investigated further the mechanism or form of the opal N contamination. However, we suspect that it derives from some of the same characteristics of diatom opal that also lead to the unique sensitivity of diatom-bound $\delta^{15}N$ to the cleaning protocol, as discussed in Section 3.1. The high effective surface area of opal and its potential for chemical and structural transformation upon heating (e.g., associated with opal dehydration) may allow for the exposure, alteration, and release of diatom-native N, as well as uptake of exogenous N species, close to the opal surface. In any case, these results indicate that heated diatom opal requires recleaning to remove adsorbed N.

As with our investigation of partial dissolution, we performed a second set of heating experiments in which an oxidative recleaning step was added after the heating treatment (right panels in Figure 4). This second experiment allowed us to further investigate: (a) the effect of N absorption into the opal, and (b) to what extent the observed changes in $\delta^{15}N$ in the different treatments involved the organic matter that remained bound within the mineral or only organic matter that could have been exposed during heating. As in the case of the dissolution experiments, any adsorbed or exposed organic material would be removed during the second oxidative cleaning, allowing us to analyze only the fraction of organic material that remained protected within the biomineral matrix. An additional motivation for this suite of experiments is that they better address the situation of fossil-bound N isotopic analysis of naturally heated samples because fossil samples are always cleaned before they are measured.

In this second set of experiments, the observed N content trends were, in general, very similar to those obtained in our first set of experiments for all fossil types, except for the diatoms (Figures 4b and 4d). These findings indicate that the additional cleaning step did not remove a substantial amount of organic matter that was exposed during heating but that remained on the surface of the fossil material. This indicates that the organic matter exposed by heating is subsequently almost completely lost from the fossil material. This is not surprising because, at temperatures >300°C, we would expect that the exposed organic material would be combusted and thus volatilized into the air.

Nevertheless, we observe a few small, but in some cases significant, differences in the $\delta^{15}N$ trends of some fossils between the "un-recleaned" and "recleaned" heating experiments. These differences suggest that some small amount of organic matter was exposed and altered during heating and was subsequently removed during the recleaning. The removed N was probably too small to be detected in our N content measurements, but its isotopic composition may

have been different enough to slightly change the δ^{15}N of the fossils in some cases. In particular, in the recleaned experiment, the δ^{15}N of the two foraminifera samples was indistinguishable from the reference in the range from 100° to 400°C, and it was only statistically different at 500°C, indicating that foraminifera calcite was stable up to 400°C. The two coral samples showed similar trends as in the un-recleaned experiment, but the difference with respect to the reference sample was smaller, particularly for the deep-sea coral. As in the un-recleaned experiments, the modern and fossil enamel samples showed no significant change in the range of temperatures analyzed, but the fossil enamel showed larger δ^{15}N increases at 400°C (0.91 ± 0.35‰) and 500°C (0.73 ± 0.31‰), suggesting that it may be less robust than modern enamel when exposed to very high temperatures. Regarding the calculated isotope effects (Figure 5), overall, they were somewhat smaller than those obtained in the un-recleaned experiment, suggesting that the values obtained in the un-recleaned experiments may slightly overestimate the fractionation induced by thermal removal of fossil-bound N. This may be due to more intense isotopic alteration of organic N that is exposed but not removed during the heating treatment. It is worth noting that the isotope effects obtained for foraminifera and corals were very low (typically <1‰), indicating that the potential biases introduced by thermal alteration would be small even if they result in significant N loss (>90%), as observed at 500°C.

In contrast to the similar trends observed for rest of the fossils in both sets of experiments, the diatom samples showed a very different pattern upon recleaning after the heating treatment. The measurements of the recleaned diatom samples suggest that the recleaning did effectively remove the adsorbed N that contaminated the samples in the first experiment. In the recleaned heating experiment, diatoms showed no significant change in N content or δ^{15}N at 100°C (Figures 4d and 4h). At 200°C, they indicated a small but statistically significant reduction in N content (15%), accompanied by a 0.92 ± 0.04‰ increase in δ^{15}N. At temperatures >200°C, the diatom sample showed the greatest decrease in N content of all the fossil types analyzed, with declines of 58% at 300°C, 94% at 400°C, and 99% at 500°C. This sharp decrease in N content was accompanied by large changes in δ^{15}N. At 300°C, diatom δ^{15}N increased with respect to the untreated control sample by 4.44 ± 0.06‰, and at 400°C, it increased by 5.46 ± 0.15‰. In contrast, at 500°C, diatoms showed a somewhat smaller increase in δ^{15}N than at 400° and 300°C, despite of the 99% decrease in its N content. Consistent with these observations, the calculated isotope effect for the diatom sample N loss varied substantially, ranging from 5.33‰ between the control sample and 300°C to 0.99‰ between the control and 500°C (Figures 5d–5f). These results may suggest the removal of different types of frustule-bound organic matter at different temperatures, with different isotopic compositions and/or different isotope effects applying to each type. However, the nearly complete loss of the initial diatom-bound N at the highest temperatures argues for caution in interpreting these results. In any case, our results suggest that the diatom-bound δ^{15}N of environmental samples exposed to temperatures above 100°C, and especially above 200°C, would likely be altered.

Overall, the patterns observed for the different fossil types indicate that both the N loss and the degree of isotopic change at different temperatures are directly linked to the robustness of the mineralogy and structure of the fossil. Thermogravimetric analysis of pretreated *Pinnularia* diatom frustules has shown that substantial sample weight loss associated with the removal of the organic fraction of the frustule starts to occur at temperatures between 200° and 300°C, and continues until 550°C, above which no further decrease in weight is detected (Van Eynde et al., 2014). Biogenic aragonite (from powdered *Acropora* corals) starts to transform to calcite at 280°C and is completely transformed to calcite at 380°C (Yoshioka & Kitano, 1985). Substantial calcite decomposition typically begins between 500° and 550°C, although marine carbonates may already become unstable at temperatures between 400° and 500°C due to the presence of magnesium (Hirota & Szyper, 1975). Tooth enamel suffers structural and chemical alteration in response to thermal stress mainly at temperatures above 600°C (Robinson & Kingston, 2020; Shipman et al., 1984).

These ranges of decomposition temperatures for opal, aragonite, calcite and enamel are consistent with the temperatures at which we start to observe substantial N loss and δ^{15}N changes in diatoms, corals, foraminifera and tooth enamel samples. The observation of significant N content and δ^{15}N changes in diatoms at 200°C and the large degrees of N loss indicate that the frustule material becomes permeable to N at high temperatures. The N loss and associated δ^{15}N change observed in coral samples at 300°C was likely associated with the conversion of aragonite to calcite. However, the smaller proportional change in N content observed between 300° and 400°C suggests that part of the coral-bound N was still trapped in the newly forming calcite. The subsequent N loss and δ^{15}N change observed at 500°C was consistent with the one observed in the calcitic foraminifera samples, and it was likely associated with the decomposition of calcite in both cases. Finally, the absence of significant changes

in N content and isotopic composition of modern enamel up to 500°C is consistent with minor alteration of the matrix at this temperature. However, the changes observed in fossil tooth enamel at 400° and 500°C suggest that aging may cause enamel to become less robust to thermal stress, at least at these extreme temperatures.

Our results, when compared to these temperatures for biomineral modification, suggest that the mineral matrix of the fossil acts as a nearly closed system with respect to N, up to the point that heating compromises the integrity of the mineral matrix itself. A previous study has shown that in *Porites* coral powder heated under aqueous conditions at 80°, 110°, and 140°C, the amino acid concentrations in the supernatant water remained within the analytical limit of detection despite of substantial changes in the chemical composition of intra-crystalline amino acids, indicating that the carbonate skeleton retained this organic N pool (Tomiak et al., 2013). Our new experiments are consistent with these observations and indicate that not only amino acids but also total N is retained within the mineral matrix at temperatures of 100°C in all the fossil types analyzed. Hence, our results indicate a negligible effect of thermal degradation on fossil-bound organic matter N isotopic composition at temperatures experienced by Cenozoic marine sediments, which are typically less than 60°C (Malinverno & Martinez, 2015). In addition, our data reveal that, in some cases (e.g., calcite or enamel), N can remain isotopically unaltered within the mineral matrix even at temperatures well above the typical combustion temperatures of protein amino acids, which range from 185° to 280°C (Weiss et al., 2018). These findings suggest that the fossil-bound N isotope method could be applied in enamel, calcitic and even aragonitic fossil samples that have suffered substantial thermal stress without significant biases in the measured $\delta^{15}N$ values. However, further work is required to fully explore this possibility.

In contrast, our experiments suggest that exposure of diatom fossils to temperatures above 100°C, and especially above 200°C, would significantly bias their N isotopic signal. Our observations may also help to explain some previous observations regarding the sensitivity of diatom-bound $\delta^{15}N$ to the cleaning protocol used. It has been noted that diatom opal from particularly opal-rich sediments, which tends to have a lower Al/Si ratio (Ren et al., 2013), has diatom-bound N that is vulnerable to $\delta^{15}N$ alteration by boiling in perchloric acid (Brunelle et al., 2007; Robinson et al., 2004). Moreover, this effect appears to be absent in diatom opal from glacial-age samples, in which the opal has a higher Al/Si ratio (Brunelle et al., 2007; Ren et al., 2013). The temperature of boiling perchloric acid is greater than 100°C, increasing with dehydration. Our temperature treatment experiments indicate that, above 100°C, diatom frustules can both lose and gain N due to thermal modification of the diatom opal. Thus, the previous findings regarding diatom cleaning may be explained by the effect of elevated treatment temperatures on the structural integrity of the diatom opal.

4. Conclusions

The results of our experiments are summarized in Figure 6, and indicate the following.

1. Fossil-bound organic matter is effectively isolated by the mineral matrix from chemical changes in the surrounding environment.
2. Fossil-bound organic matter is removed without isotopic discrimination by partial dissolution of the mineral matrix.
3. In the fossil types investigated, fossil-bound organic matter has a relatively uniform N isotopic composition across the mineral matrix.
4. The fossil-native organic matter exposed by acid dissolution remains, at least in part, as a physicochemical framework connected with the remaining biomineral. If recrystallization occurs at a scale that minimizes exposure of this organic N to microbes, our observations offer a possible explanation for the apparent stability of fossil-bound organic matter in recrystallized biominerals (e.g., Kast et al., 2019).
5. During heating, the mineral matrix behaves as a nearly closed system with respect to N, up to the point that the high temperature compromises the integrity of the mineral matrix itself.

Thus, our results provide strong experimental support for the robustness of fossil-bound organic matter to reconstruct the original N isotopic composition of ancient organisms. We acknowledge that the full range of diagenetic reactions found in the environment on geological timescales are difficult to simulate in the laboratory. Thus, direct observations from the geologic past are also necessary to provide a more complete assessment of the potential diagenetic effects on fossil-bound organic matter. In this vein, the results obtained here are consistent with observations from the geologic past. First, a number of studies have shown that the N content of fossils of the same species/genus remains relatively stable across thousands to millions of years, suggesting that mineral
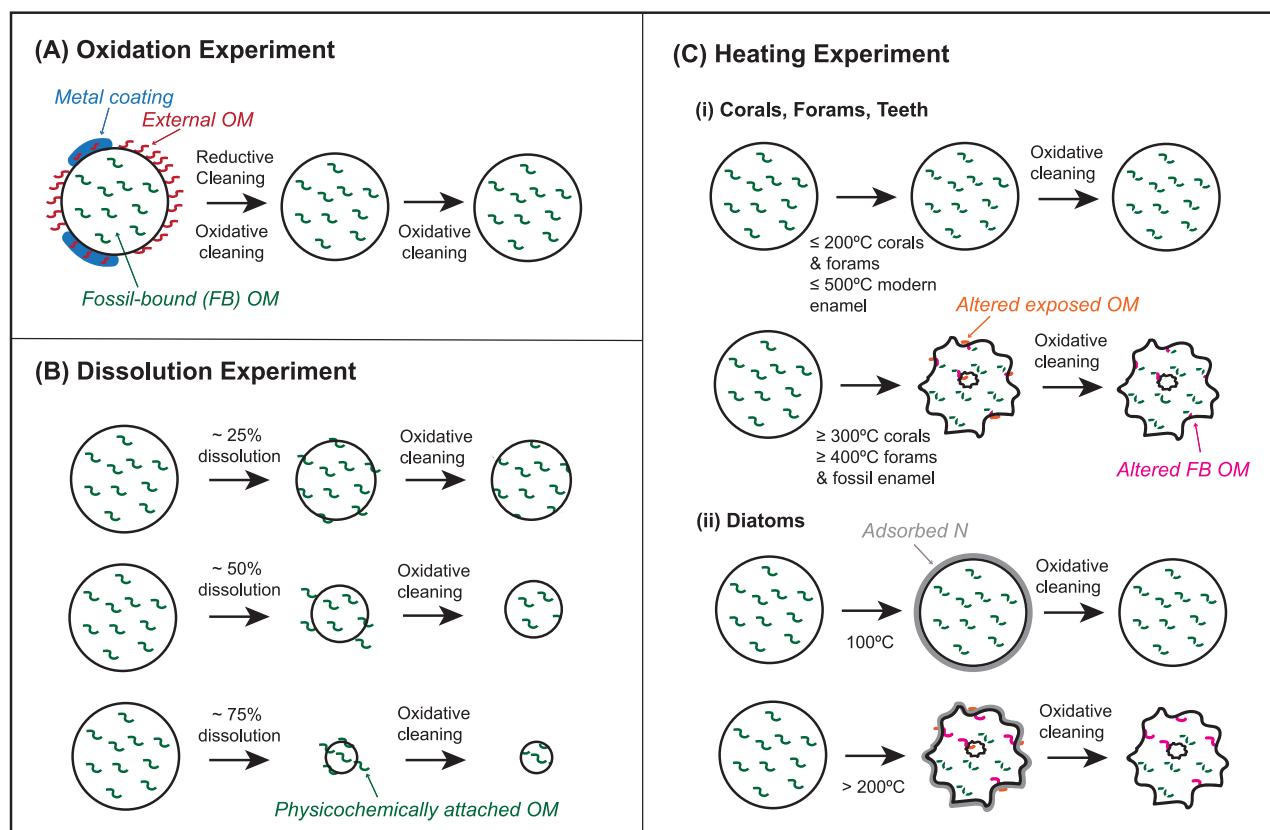
Figure 6. Summary of the interpretation of the oxidation, dissolution and heating experiments. (a) In our oxidation experiments, our reductive + oxidative cleaning causes a substantial reduction in N content and a change in $\delta^{15}N$ that is consistent for a given standard but varies among different standards and fossil types (Figures 2c and 2d). We interpret these changes to reflect the removal of external OM (red lines). However, the oxidative recleaning did not produce any significant changes in N content or $\delta^{15}N$, indicating that FB-OM (green lines) was effectively protected by the biomineral from chemical attack. (b) Our dissolution experiments reveal a progressive increase in N content per mg of calcite as dissolution increased (Figure 3c). This change in N content occurred without substantial change in $\delta^{15}N$ (Figure 3g). The progressive increase in N disappeared after an additional oxidative cleaning (Figure 3d), without substantial change in $\delta^{15}N$ (Figure 3h). These results indicate that part of the FB-OM was exposed after dissolution, but it was not altered, and it remained physiochemically attached to the biomineral (exposed green lines). This OM was not removed during rinsing with Milli-Q water, but it was completely eliminated with an oxidative recleaning. The stability of the $\delta^{15}N$ values obtained before and after the recleaning demonstrate that FB-OM has a relatively homogenous isotopic composition, and that it was not altered during the dissolution process. (c) Our results indicate no significant changes in FB N content or $\delta^{15}N$ at temperatures $\leq 200°C$ in any of the corals, foraminifera or teeth analyzed, regardless of whether samples underwent oxidative recleaning (Figures 4c,4d,4g and 4h). These results indicate that, despite potential changes in the molecular structure of the FB-OM (dashing of the green lines) that could be induced by heating (Tomiak et al., 2013), the biomineral acted as a closed system with respect to N. Corals showed substantial N content changes at temperatures $\geq 300°C$, foraminifera and fossil enamel at $\geq 400°C$, while modern enamel remained stable even at 500°C. Despite these substantial changes in N content, after oxidative recleaning, the $\delta^{15}N$ of corals, foraminifera and fossil teeth showed minimal changes (Figure 4h). This suggests that the proportion of FB-OM that had been altered so as to lose a portion of its N to external environment but remained in the samples (pink lines) was very small. Diatoms show a very different response to heating than the rest of the fossils. When they were not oxidatively recleaned after heating, N content increased and $\delta^{15}N$ decreased significantly (Figures 4c and 4g), suggesting contamination of the samples by adsorption of N during heating. This contamination was successfully removed by recleaning (Figure 4d). In contrast to the other fossil types, in diatoms, substantial N loss was observed even at temperatures $\geq 200°C$, and it was associated with substantial $\delta^{15}N$ changes (Figures 4c and 4g). These findings suggest the presence of a larger proportion of altered FB-OM (pink lines) in diatoms than in other fossil after heating. Overall, our results indicate that thermal N loss depends on the resistance of the biomineral itself to thermal stress. The potential alteration of FB-OM was significant for diatoms at temperatures $\geq 200°C$, due to the thermal sensitivity of diatom opal, while higher temperature thresholds were observed for corals, foraminifera and tooth enamel.

matrix acted as a closed system with respect to N (Kast et al., 2019; Leichliter et al., 2021; Ren et al., 2017; Studer et al., 2012). This observation is consistent with our findings indicating a similar behavior for fossil and modern enamel across the different experiments, suggesting that aging may not affect substantially the robustness of the mineral matrix, except perhaps at extreme temperatures (i.e., above 400°C). Second, different species of foraminifera, which have different sensitivities to alteration of the mineral matrix, reveal consistent $\delta^{15}N$ records (Ren et al., 2015, 2017; Straub et al., 2013). Third, foraminifera, corals and diatoms, which have different sensitivities to alteration, provide consistent estimates of regional $\delta^{15}N$ changes when measured across the same

time periods and in the same regions (Ai et al., 2020; Martinez-Garcia et al., 2014; Studer et al., 2015; Wang et al., 2017).

The evidence, reported here and previously, for the robustness of fossil-bound N has implications from prior comparisons of fossil-bound and bulk sediment $\delta^{15}N$, which often shows dramatic differences (Martinez-Garcia et al., 2014; Ren et al., 2017; Robinson et al., 2005; Straub et al., 2013; Studer et al., 2021). Bulk sediment $\delta^{15}N$ is known to be sensitive to diagenetic alteration and contamination by terrestrial N inputs (Robinson et al., 2012). In contrast, so long as the diagenetic conditions are appropriate to preserve the biomineral in question, fossil-bound $\delta^{15}N$ appears to be remarkably robust. Even in situations of biomineral dissolution/recrystallization, such as in early Cenozoic, carbonate-rich deep-sea sediments, N content and $\delta^{15}N$ data indicate the preservation of fossil-bound N (Kast et al., 2019), which is consistent with the results of the dissolution experiments presented here. Thus, the comparison of fossil-bound and bulk sediment $\delta^{15}N$ could offer insights into diagenetic processes affecting sedimentary organic matter (Martinez-Garcia et al., 2014), or into changes in terrestrial N inputs (Ren et al., 2009, 2017; Straub et al., 2013). Alternatively, if one seeks to argue that the fossil-bound N is "to blame" for a disagreement with bulk sediment $\delta^{15}N$, or if differences in fossil-bound-$\delta^{15}N$ are found among different fossil types or species, one must look to the biological controls on the isotopic signatures incorporated into fossil-bound organic matter by the fossil-producing organisms. This situation motivates an expansion of ground-truthing research that focuses on the biological and ecological controls on the N encapsulated within different types of newly generated biominerals.

Data Availability Statement

All the data generated in this study are available in the Supporting Information, and in Zenodo (https://doi.org/10.5281/zenodo.6884681).

References

Ai, X. E., Studer, A. S., Sigman, D. M., Martínez-García, A., Fripiat, F., Thöle, L. M., et al. (2020). Southern Ocean upwelling, Earth's obliquity, and glacial-interglacial atmospheric CO_2 change. *Science*, *370*(6522), 1348–1352. https://doi.org/10.1126/science.abd2115

Altabet, M. A., & Curry, W. B. (1989). Testing models of past ocean chemistry using foraminifera $^{15}N/^{14}N$. *Global Biogeochemical Cycles*, *3*(2), 107–119. https://doi.org/10.1029/GB003i002p00107

Arndt, S., Jørgensen, B. B., LaRowe, D. E., Middelburg, J. J., Pancost, R. D., & Regnier, P. (2013). Quantifying the degradation of organic matter in marine sediments: A review and synthesis. *Earth-Science Reviews*, *123*, 53–86. https://doi.org/10.1016/j.earscirev.2013.02.008

Bada, J. L., Schoeninger, M. J., & Schimmelmann, A. (1989). Isotopic fractionation during peptide bond hydrolysis. *Geochimica et Cosmochimica Acta*, *53*(12), 3337–3341. https://doi.org/10.1016/0016-7037(89)90114-2

Bai, Y., Yu, Z., Ackerman, L., Zhang, Y., Bonde, J., Li, W., et al. (2020). Protein nanoribbons template enamel mineralization. *Proceedings of the National Academy of Sciences of the United States of America*, *117*(32), 19201–19208. https://doi.org/10.1073/pnas.2007838117

Braman, R. S., & Hendrix, S. A. (2002). Nanogram nitrite and nitrate determination in environmental and biological materials by vanadium(III) reduction with chemiluminescence detection. *Analytical Chemistry*, *61*(24), 2715–2718. https://doi.org/10.1021/ac00199a007

Bridoux, M. C., Annenkov, V. V., Keil, R. G., & Ingalls, A. E. (2012). Widespread distribution and molecular diversity of diatom frustule bound aliphatic long chain polyamines (LCPAs) in marine sediments. *Organic Geochemistry*, *48*, 9–20. https://doi.org/10.1016/j.orggeochem.2012.04.002

Bridoux, M. C., Keil, R. G., & Ingalls, A. E. (2012). Analysis of natural diatom communities reveals novel insights into the diversity of long chain polyamine (LCPA) structures involved in silica precipitation. *Organic Geochemistry*, *47*, 9–21. https://doi.org/10.1016/j.orggeochem.2012.02.010

Brown, S. J., & Elderfield, H. (1996). Variations in Mg/Ca and Sr/Ca ratios of planktonic foraminifera caused by postdepositional dissolution: Evidence of shallow Mg-dependent dissolution. *Paleoceanography*, *11*(5), 543–551. https://doi.org/10.1029/96pa01491

Brunelle, B. G., Sigman, D. M., Cook, M. S., Keigwin, L. D., Haug, G. H., Plessen, B., et al. (2007). Evidence from diatom-bound nitrogen isotopes for subarctic Pacific stratification during the last ice age and a link to North Pacific denitrification changes. *Paleoceanography*, *22*(1). PA1215. https://doi.org/10.1029/2005pa001205

Burdige, D. J. (2006). *Geochemistry of marine sediments*. Princeton University Press.

Cappellini, E., Welker, F., Pandolfi, L., Ramos-Madrigal, J., Samodova, D., Rüther, P. L., et al. (2019). Early Pleistocene enamel proteome from Dmanisi resolves Stephanorhinus phylogeny. *Nature*, *574*(7776), 103–107. https://doi.org/10.1038/s41586-019-1555-y

Casciotti, K. L. (2016). Nitrogen and oxygen isotopic studies of the marine nitrogen cycle. *Annual Review of Marine Science*, *8*(1), 379–407. https://doi.org/10.1146/annurev-marine-010213-135052

Castiblanco, G. A., Rutishauser, D., Ilag, L. L., Martignon, S., Castellanos, J. E., & Mejía, W. (2015). Identification of proteins from human permanent erupted enamel. *European Journal of Oral Sciences*, *123*(6), 390–395. https://doi.org/10.1111/eos.12214

Chanda, P., Gorski, C. A., Oakes, R. L., & Fantle, M. S. (2019). Low temperature stable mineral recrystallization of foraminiferal tests and implications for the fidelity of geochemical proxies. *Earth and Planetary Science Letters*, *506*, 428–440. https://doi.org/10.1016/j.epsl.2018.11.011

Cowie, G. L., & Hedges, J. I. (1994). Biochemical indicators of diagenetic alteration in natural organic matter mixtures. *Nature*, *369*(6478), 304–307. https://doi.org/10.1038/369304a0

Cuif, J.-P., & Dauphin, Y. (2005). The two-step mode of growth in the scleractinian coral skeletons from the micrometre to the overall scale. *Journal of Structural Biology*, *150*(3), 319–331. https://doi.org/10.1016/j.jsb.2005.03.004

Cusack, M., & Freer, A. (2008). Biomineralization: Elemental and organic influence in carbonate systems. *Chemical Reviews*, *108*(11), 4433–4454. https://doi.org/10.1021/cr078270o

Dauwe, B., & Middelburg, J. J. (1998). Amino acids and hexosamines as indicators of organic matter degradation state in North Sea sediments. *Limnology & Oceanography*, *43*(5), 782–798. https://doi.org/10.4319/lo.1998.43.5.0782

Deniro, M. J., & Epstein, S. (1981). Influence of diet on the distribution of nitrogen isotopes in animals. *Geochimica et Cosmochimica Acta*, *45*(3), 341–351. https://doi.org/10.1016/0016-7037(81)90244-1

Duprey, N. N., Wang, X. T., Kim, T., Cybulski, J. D., Vonhof, H. B., Crutzen, P. J., et al. (2020). Megacity development and the demise of coastal coral communities: Evidence from coral skeleton δ15N records in the Pearl River Estuary. *Global Change Biology*, *26*(3), 1338–1353. https://doi.org/10.1111/gcb.14923

Engel, M. H., Goodfriend, G. A., Qian, Y. R., & Macko, S. A. (1994). Indigeneity of organic-matter in fossils–A test using stable-isotope analysis of amino-acid enantiomers in quaternary Mollusk shells. *Proceedings of the National Academy of Sciences of the United States of America*, *91*(22), 10475–10478. https://doi.org/10.1073/pnas.91.22.10475

Engel, M. H., & Macko, S. A. (1986). Stable isotope evaluation of the origins of amino-acids in fossils. *Nature*, *323*(6088), 531–533. https://doi.org/10.1038/323531a0

Erler, D. V., Farid, H. T., Glaze, T. D., Carlson-Perret, N. L., & Lough, J. M. (2020). Coral skeletons reveal the history of nitrogen cycling in the coastal Great Barrier Reef. *Nature Communications*, *11*(1), 1500. https://doi.org/10.1038/s41467-020-15278-w

Erler, D. V., Wang, X. C. T., Sigman, D. M., Scheffers, S. R., Martinez-Garcia, A., & Haug, G. H. (2016). Nitrogen isotopic composition of organic matter from a 168 year-old coral skeleton: Implications for coastal nutrient cycling in the Great Barrier Reef Lagoon. *Earth and Planetary Science Letters*, *434*, 161–170. https://doi.org/10.1016/j.epsl.2015.11.023

Farmer, J. R., Sigman, D. M., Granger, J., Underwood, O. M., Fripiat, F., Cronin, T. M., et al. (2021). Arctic Ocean stratification set by sea level and freshwater inputs since the last ice age. *Nature Geoscience*, *14*(9), 684–689. https://doi.org/10.1038/s41561-021-00789-y

Frankowiak, K., Mazur, M., Gothmann, A. M., & Stolarski, J. (2013). Diagenetic alteration of Triassic coral from the aragonite Konservat-Lagerstatte in Alakir Cay, Turkey: Implications for geochemical measurements. *PALAIOS*, *28*(6), 333–342. https://doi.org/10.2110/palo.2012.p12-116r

Freudenthal, T., Wagner, T., Wenzhöfer, F., Zabel, M., & Wefer, G. (2001). Early diagenesis of organic matter from sediments of the eastern subtropical Atlantic: Evidence from stable nitrogen and carbon isotopes. *Geochimica et Cosmochimica Acta*, *65*(11), 1795–1808. https://doi.org/10.1016/s0016-7037(01)00554-3

Fripiat, F., Martínez-García, A., Fawcett, S. E., Kemeny, P. C., Studer, A. S., Smart, S. M., et al. (2019). The isotope effect of nitrate assimilation in the Antarctic Zone: Improved estimates and paleoceanographic implications. *Geochimica et Cosmochimica Acta*, *247*, 261–279. https://doi.org/10.1016/j.gca.2018.12.003

Fripiat, F., Martínez-García, A., Marconi, D., Fawcett, S. E., Kopf, S. H., Luu, V. H., et al. (2021). Nitrogen isotopic constraints on nutrient transport to the upper ocean. *Nature Geoscience*, *14*(11), 855–861. https://doi.org/10.1038/s41561-021-00836-8

Gehler, A., Tutken, T., & Pack, A. (2012). Oxygen and carbon isotope variations in a modern rodent community–Implications for palaeoenvironmental reconstructions. *PLoS One*, *7*(11), e49531. https://doi.org/10.1371/journal.pone.0049531

Hirota, J., & Szyper, J. P. (1975). Separation of total particulate carbon into inorganic and organic components. *Limnology & Oceanography*, *20*(5), 896–900. https://doi.org/10.4319/lo.1975.20.5.0896

Ingalls, A. E., Lee, C., & Druffel, E. R. M. (2003). Preservation of organic matter in mound-forming coral skeletons. *Geochimica et Cosmochimica Acta*, *67*(15), 2827–2841. https://doi.org/10.1016/S0016-7037(03)00079-6

Kast, E. R. (2020). *Development and application of biogenic mineral-bound nitrogen isotope measurements to the million-year timescale*. Geosciences Department. Princeton University.

Kast, E. R., Griffiths, M. L., Kim, S. L., Rao, Z. C., Shimada, K., Becker, M. A., et al. (2022). Cenozoic megatooth sharks occupied extremely high trophic positions. *Science Advances*, *8*(25). https://doi.org/10.1126/sciadv.abl6529

Kast, E. R., Stolper, D. A., Auderset, A., Higgins, J. A., Ren, H., Wang, X. T., et al. (2019). Nitrogen isotope evidence for expanded ocean suboxia in the early Cenozoic. *Science*, *364*(6438), 386–389. https://doi.org/10.1126/science.aau5784

Killingley, J. S. (1983). Effects of diagenetic recrystallization on 18O/16O values of deep-sea sediments. *Nature*, *301*(5901), 594–597. https://doi.org/10.1038/301594a0

Knapp, A. N., Sigman, D. M., & Lipschultz, F. (2005). N isotopic composition of dissolved organic nitrogen and nitrate at the Bermuda Atlantic time-series study site. *Global Biogeochemical Cycles*, *19*(1). Gb1018. https://doi.org/10.1029/2004gb002320

Kroger, N., Deutzmann, R., Bergsdorf, C., & Sumper, M. (2000). Species-specific polyamines from diatoms control silica morphology. *Proceedings of the National Academy of Sciences of the United States of America*, *97*(26), 14133–14138. https://doi.org/10.1073/pnas.260496497

Kroger, N., Lorenz, S., Brunner, E., & Sumper, M. (2002). Self-assembly of highly phosphorylated silaffins and their function in Biosilica Morphogenesis. *Science*, *298*(5593), 584–586. https://doi.org/10.1126/science.1076221

Kullmer, O. (2008). The fossil suidae from the plio-pleistocene Chiwondo Beds of northern Malawi, Africa. *Journal of Vertebrate Paleontology*, *28*(1), 208–216. https://doi.org/10.1671/0272-4634(2008)28[208:tfsftp]2.0.co;2

Leichliter, J. N., Lüdecke, T., Foreman, A. D., Duprey, N. N., Winkler, D. E., Kast, E. R., et al. (2021). Nitrogen isotopes in tooth enamel record diet and trophic level enrichment: Results from a controlled feeding experiment. *Chemical Geology*, *563*, 120047. https://doi.org/10.1016/j.chemgeo.2020.120047

Lueders-Dumont, J. A., Wang, X. T., Jensen, O. P., Sigman, D. M., & Ward, B. B. (2018). Nitrogen isotopic analysis of carbonate-bound organic matter in modern and fossil fish otoliths. *Geochimica et Cosmochimica Acta*, *224*, 200–222. https://doi.org/10.1016/j.gca.2018.01.001

Malinverno, A., & Martinez, E. A. (2015). The effect of temperature on organic carbon degradation in marine sediments. *Scientific Reports*, *5*(1), 17861. https://doi.org/10.1038/srep17861

Martinez-Garcia, A., Sigman, D. M., Ren, H. J., Anderson, R. F., Straub, M., Hodell, D. A., et al. (2014). Iron fertilization of the subantarctic ocean during the last ice age. *Science*, *343*(6177), 1347–1350. https://doi.org/10.1126/science.1246848

McCorkle, D. C., Martin, P. A., Lea, D. W., & Klinkhammer, G. P. (1995). Evidence of a dissolution effect on benthic foraminiferal shell chemistry: δ13C, Cd/Ca, Ba/Ca, and Sr/Ca results from the Ontong Java Plateau. *Paleoceanography*, *10*(4), 699–714. https://doi.org/10.1029/95pa01427

Mehra, O. P., & Jackson, M. L. (1958). Iron oxide removal from soils and clays by a dithionite–citrate system buffered with sodium bicarbonate. *Clays and Clay Minerals*, *7*(1), 317–327. https://doi.org/10.1346/CCMN.1958.0070122

Morales, L. V., Sigman, D. M., Horn, M. G., & Robinson, R. S. (2013). Cleaning methods for the isotopic determination of diatom-bound nitrogen in non-fossil diatom frustules. *Limnology and Oceanography: Methods*, *11*(2), 101–112. https://doi.org/10.4319/lom.2013.11.101

Pearson, P. N. (2017). Oxygen isotopes in foraminifera: Overview and historical review. *Paleontological Society Papers*, *18*, 1–38. https://doi.org/10.1017/s1089332600002539

Pearson, P. N., Ditchfield, P. W., Singano, J., Harcourt-Brown, K. G., Nicholas, C. J., Olsson, R. K., et al. (2001). Warm tropical sea surface temperatures in the Late Cretaceous and Eocene epochs. *Nature*, *413*(6855), 481–487. https://doi.org/10.1038/35097000

Pearson, P. N., van Dongen, B. E., Nicholas, C. J., Pancost, R. D., Schouten, S., Singano, J. M., & Wade, B. S. (2007). Stable warm tropical climate through the Eocene Epoch. *Geology*, *35*(3), 211. https://doi.org/10.1130/g23175a.1

Rejebian, V. A., Harris, A. G., & Huebner, J. S. (1987). Conodont color and textural alteration: An index to regional metamorphism, contact metamorphism, and hydrothermal alteration. *The Geological Society of America Bulletin*, *99*(4), 471. https://doi.org/10.1130/0016-7606(1987)99<471:ccataa>2.0.co;2

Ren, H. (2010). *Developement and paleoceanographic application of plancktonic foraminifera-bound nitrogen isotopes*. Department of Geoscience. Princeton University.

Ren, H., Sigman, D. M., Martínez-García, A., Anderson, R. F., Chen, M.-T., Ravelo, A. C., et al. (2017). Impact of glacial/interglacial sea level change on the ocean nitrogen cycle. *Proceedings of the National Academy of Sciences of the United States of America*, *114*(33), E6759–E6766. https://doi.org/10.1073/pnas.1701315114

Ren, H., Sigman, D. M., Meckler, A. N., Plessen, B., Robinson, R. S., Rosenthal, Y., & Haug, G. H. (2009). Foraminiferal isotope evidence of reduced nitrogen fixation in the ice age Atlantic Ocean. *Science*, *323*(5911), 244–248. https://doi.org/10.1126/science.1165787

Ren, H. J., Brunelle, B. G., Sigman, D. M., & Robinson, R. S. (2013). Diagenetic aluminum uptake into diatom frustules and the preservation of diatom-bound organic nitrogen. *Marine Chemistry*, *155*, 92–101. https://doi.org/10.1016/j.marchem.2013.05.016

Ren, H. J., Studer, A. S., Serno, S., Sigman, D. M., Winckler, G., Anderson, R. F., et al. (2015). Glacial-to-interglacial changes in nitrate supply and consumption in the subarctic North Pacific from microfossil-bound N isotopes at two trophic levels. *Paleoceanography*, *30*(9), 1217–1232. https://doi.org/10.1002/2014pa002765

Roach, D., & Gehrke, C. W. (1970). The hydrolysis of proteins. *Journal of Chromatography A*, *52*, 393–404. https://doi.org/10.1016/s0021-9673(01)96589-6

Robinson, J. R., & Kingston, J. D. (2020). Burned by the fire: Isotopic effects of experimental combustion of faunal tooth enamel. *Journal of Archaeological Science: Reports*, *34*, 102593. https://doi.org/10.1016/j.jasrep.2020.102593

Robinson, R. S., Brunelle, B. G., & Sigman, D. M. (2004). Revisiting nutrient utilization in the glacial Antarctic: Evidence from a new method for diatom-bound N isotopic analysis. *Paleoceanography*, *19*(3). PA3001. https://doi.org/10.1029/2003pa000996

Robinson, R. S., Kienast, M., Luiza Albuquerque, A., Altabet, M., Contreras, S., De Pol Holz, R., et al. (2012). A review of nitrogen isotopic alteration in marine sediments. *Paleoceanography*, *27*(4). PA4203. https://doi.org/10.1029/2012pa002321

Robinson, R. S., Sigman, D. M., DiFiore, P. J., Rohde, M. M., Mashiotta, T. A., & Lea, D. W. (2005). Diatom-bound N-15/N-14: New support for enhanced nutrient consumption in the ice age subantarctic. *Paleoceanography*, *20*(3). https://doi.org/10.1029/2004pa001114

Rosenthal, Y., Lohmann, G. P., Lohmann, K. C., & Sherrell, R. M. (2000). Incorporation and preservation of Mg in Globigerinoides Sacculifer: Implications for reconstructing the temperature and ^{18}O/^{16}O of seawater. *Paleoceanography*, *15*(1), 135–145. https://doi.org/10.1029/1999pa000415

Schroeder, R. A. (1975). Absence of *β*-alanine and *γ*-aminobutyric acid in cleaned foraminiferal shells: Implications for use as a chemical criterion to indicate removal of non-indigenous amino acid contaminants. *Earth and Planetary Science Letters*, *25*(3), 274–278. https://doi.org/10.1016/0012-821x(75)90241-1

Shemesh, A., Macko, S. A., Charles, C. D., & Rau, G. H. (1993). Isotopic evidence for reduced productivity in the glacial Southern Ocean. *Science*, *262*(5132), 407–410. https://doi.org/10.1126/science.262.5132.407

Shipman, P., Foster, G., & Schoeninger, M. (1984). Burnt bones and teeth–An experimental-study of color, morphology, crystal-structure and shrinkage. *Journal of Archaeological Science*, *11*(4), 307–325. https://doi.org/10.1016/0305-4403(84)90013-X

Sigman, D. M., Altabet, M. A., Francois, R., McCorkle, D. C., & Gaillard, J. F. (1999). The isotopic composition of diatom-bound nitrogen in Southern Ocean sediments. *Paleoceanography*, *14*(2), 118–134. https://doi.org/10.1029/1998pa900018

Sigman, D. M., Casciotti, K. L., Andreani, M., Barford, C., Galanter, M., & Bohlke, J. K. (2001). A bacterial method for the nitrogen isotopic analysis of nitrate in seawater and freshwater. *Analytical Chemistry*, *73*(17), 4145–4153. https://doi.org/10.1021/ac010088e

Sigman, D. M., & Fripiat, F. (2019). *Nitrogen isotopes in the ocean* (pp. 263–278). Encyclopedia of Ocean Sciences.

Sigman, D. M., Fripiat, F., Studer, A. S., Kemeny, P. C., Martínez-García, A., Hain, M. P., et al. (2021). The Southern Ocean during the ice ages: A review of the Antarctic surface isolation hypothesis, with comparison to the North Pacific. *Quaternary Science Reviews*, *254*, 106732. https://doi.org/10.1016/j.quascirev.2020.106732

Smart, S. M., Ren, H., Fawcett, S. E., Schiebel, R., Conte, M., Rafter, P. A., et al. (2018). Ground-truthing the planktic foraminifer-bound nitrogen isotope paleo-proxy in the Sargasso Sea. *Geochimica et Cosmochimica Acta*, *235*, 463–482. https://doi.org/10.1016/j.gca.2018.05.023

Smith, A. C., Leng, M. J., Swann, G. E. A., Barker, P. A., Mackay, A. W., Ryves, D. B., et al. (2016). An experiment to assess the effects of diatom dissolution on oxygen isotope ratios. *Rapid Communications in Mass Spectrometry*, *30*(2), 293–300. https://doi.org/10.1002/rcm.7446

Stolarski, J. (2003). Three-dimensional micro- and nanostructural characteristics of the scleractinian coral skeleton: A biocalcification proxy. *Acta Palaeontologica Polonica*, *48*, 497–530.

Straub, M. (2012). *Application of foraminifera-bound nitrogen isotopes to Atlantic paleoceanography*. Earth Science Department. ETH Zurich.

Straub, M., Sigman, D. M., Auderset, A., Ollivier, J., Petit, B., Hinnenberg, B., et al. (2021). Distinct nitrogen isotopic compositions of healthy and cancerous tissue in mice brain and head&neck micro-biopsies. *BMC Cancer*, *21*(1), 805. https://doi.org/10.1186/s12885-021-08489-x

Straub, M., Sigman, D. M., Ren, H., Martinez-Garcia, A., Meckler, A. N., Hain, M. P., & Haug, G. H. (2013). Changes in North Atlantic nitrogen fixation controlled by ocean circulation. *Nature*, *501*(7466), 200–203. https://doi.org/10.1038/nature12397

Studer, A. S., Martinez-Garcia, A., Jaccard, S. L., Girault, F. E., Sigman, D. M., & Haug, G. H. (2012). Enhanced stratification and seasonality in the Subarctic Pacific upon Northern Hemisphere Glaciation-New evidence from diatom-bound nitrogen isotopes, alkenones and archaeal tetraethers. *Earth and Planetary Science Letters*, *351*, 84–94. https://doi.org/10.1016/j.epsl.2012.07.029

Studer, A. S., Mekik, F., Ren, H., Hain, M. P., Oleynik, S., Martínez-García, A., et al. (2021). Ice age-holocene similarity of foraminifera-bound nitrogen isotope ratios in the eastern equatorial Pacific. *Paleoceanography and Paleoclimatology*, *36*(5). e2020PA004063. https://doi.org/10.1029/2020pa004063

Studer, A. S., Sigman, D. M., Martinez-Garcia, A., Benz, V., Winckler, G., Kuhn, G., et al. (2015). Antarctic Zone nutrient conditions during the last two glacial cycles. *Paleoceanography*, *30*(7), 845–862. https://doi.org/10.1002/2014PA002745

Studer, A. S., Sigman, D. M., Martínez-García, A., Thöle, L. M., Michel, E., Jaccard, S. L., et al. (2018). Increased nutrient supply to the Southern Ocean during the Holocene and its implications for the pre-industrial atmospheric CO_2 rise. *Nature Geoscience*, *11*(10), 756–760. https://doi.org/10.1038/s41561-018-0191-8

Sulpis, O., Jeansson, E., Dinauer, A., Lauvset, S. K., & Middelburg, J. J. (2021). Calcium carbonate dissolution patterns in the ocean. *Nature Geoscience*, *14*(6), 423–428. https://doi.org/10.1038/s41561-021-00743-y

Swart, K. A., Oleynik, S., Martínez-García, A., Haug, G. H., & Sigman, D. M. (2021). Correlation between the carbon isotopic composition of planktonic foraminifera-bound organic matter and surface water pCO$_2$ across the equatorial Pacific. *Geochimica et Cosmochimica Acta*, *306*, 281–303. https://doi.org/10.1016/j.gca.2021.03.007

Tomiak, P. J., Penkman, K. E. H., Hendy, E. J., Demarchi, B., Murrells, S., Davis, S. A., et al. (2013). Testing the limitations of artificial protein degradation kinetics using known-age massive Porites coral skeletons. *Quaternary Geochronology*, *16*, 87–109. https://doi.org/10.1016/j.quageo.2012.07.001

van Cappellen, P., Dixit, S., & van Beusekom, J. (2002). Biogenic silica dissolution in the oceans: Reconciling experimental and field-based dissolution rates. *Global Biogeochemical Cycles*, *16*(4), 23-1–23-10. https://doi.org/10.1029/2001gb001431

van Eynde, E., Lenaerts, B., Tytgat, T., Verbruggen, S. W., Hauchecorne, B., Blust, R., & Lenaerts, S. (2014). Effect of pretreatment and temperature on the properties of Pinnularia biosilica frustules. *RSC Advances*, *4*(99), 56200–56206. https://doi.org/10.1039/c4ra09305d

Wang, X. C. T., Prokopenko, M. G., Sigman, D. M., Adkins, J. F., Robinson, L. F., Ren, H. J., et al. (2014). Isotopic composition of carbonate-bound organic nitrogen in deep-sea scleractinian corals: A new window into past biogeochemical change. *Earth and Planetary Science Letters*, *400*, 243–250. https://doi.org/10.1016/j.epsl.2014.05.048

Wang, X. T., Sigman, D. M., Cohen, A. L., Sinclair, D. J., Sherrell, R. M., Cobb, K. M., et al. (2016). Influence of open ocean nitrogen supply on the skeletal delta N-15 of modern shallow-water Scleractinian corals. *Earth and Planetary Science Letters*, *441*, 125–132. https://doi.org/10.1016/j.epsl.2016.02.032

Wang, X. T., Sigman, D. M., Cohen, A. L., Sinclair, D. J., Sherrell, R. M., Weigand, M. A., et al. (2015). Isotopic composition of skeleton-bound organic nitrogen in reef-building symbiotic corals: A new method and proxy evaluation at Bermuda. *Geochimica et Cosmochimica Acta*, *148*, 179–190. https://doi.org/10.1016/j.gca.2014.09.017

Wang, X. T., Sigman, D. M., Prokopenko, M. G., Adkins, J. F., Robinson, L. F., Hines, S. K., et al. (2017). Deep-sea coral evidence for lower Southern Ocean surface nitrate concentrations during the last ice age. *Proceedings of the National Academy of Sciences of the United States of America*, *114*(13), 3352–3357. https://doi.org/10.1073/pnas.1615718114

Weigand, M. A., Foriel, J., Barnett, B., Oleynik, S., & Sigman, D. M. (2016). Updates to instrumentation and protocols for isotopic analysis of nitrate by the denitrifier method. *Rapid Communications in Mass Spectrometry*, *30*(12), 1365–1383. https://doi.org/10.1002/rcm.7570

Weiner, S., & Erez, J. (1984). Organic matrix of the shell of the foraminifer, Heterostegina depressa. *Journal of Foraminiferal Research*, *14*(3), 206–212. https://doi.org/10.2113/gsjfr.14.3.206

Weiss, I. M., Muth, C., Drumm, R., & Kirchner, H. O. K. (2018). Thermal decomposition of the amino acids glycine, cysteine, aspartic acid, asparagine, glutamic acid, glutamine, arginine and histidine. *BMC Biophysics*, *11*(1), 2. https://doi.org/10.1186/s13628-018-0042-4

Whelan, J. K. (1977). Amino acids in a surface sediment core of the Atlantic abyssal plain. *Geochimica et Cosmochimica Acta*, *41*(6), 803–810. https://doi.org/10.1016/0016-7037(77)90050-3

Wolf, N., Carleton, S. A., & Martínez del Rio, C. (2009). Ten years of experimental animal isotopic ecology. *Functional Ecology*, *23*(1), 17–26. https://doi.org/10.1111/j.1365-2435.2009.01529.x

Yoshioka, S., & Kitano, Y. (1985). Transformation of aragonite to calcite through heating. *Geochemistry Journal*, *19*(4), 245–249. https://doi.org/10.2343/geochemj.19.245

Zheng, Y., Anderson, R. F., Froelich, P. N., Beck, W., McNichol, A. P., & Guilderson, T. (2002). Challenges in radiocarbon dating organic carbon in opal-rich marine sediments. *Radiocarbon*, *44*(1), 123–136. https://doi.org/10.1017/s0033822200064729